

# Persistent Amyloidosis following Suppression of A $\beta$ Production in a Transgenic Model of Alzheimer Disease

Joanna L. Jankowsky<sup>1,2\*</sup>, Hilda H. Slunt<sup>1‡</sup>, Victoria Gonzales<sup>1</sup>, Alena V. Savonenko<sup>1</sup>, Jason C. Wen<sup>3</sup>, Nancy A. Jenkins<sup>4</sup>, Neal G. Copeland<sup>4</sup>, Linda H. Younkin<sup>5</sup>, Henry A. Lester<sup>2</sup>, Steven G. Younkin<sup>5</sup>, David R. Borchelt<sup>1,6\*‡</sup>

**1** Department of Pathology, The Johns Hopkins University School of Medicine, Baltimore, Maryland, United States of America, **2** Division of Biology, California Institute of Technology, Pasadena, California, United States of America, **3** Department of Cell Biology, The Johns Hopkins University School of Medicine, Baltimore, Maryland, United States of America, **4** Mouse Cancer Genetics Program, National Cancer Institute Frederick Cancer Research and Development Center, Frederick, Maryland, United States of America, **5** Mayo Clinic Jacksonville, Jacksonville, Florida, United States of America, **6** Department of Neuroscience, The Johns Hopkins University School of Medicine, Baltimore, Maryland, United States of America

**Competing Interests:** The authors have declared that no competing interests exist.

**Author Contributions:** JJ and DRB designed the study and wrote the manuscript; JJ, HHS, VG, JCW, LHY, SGY and DRB performed experiments; NAJ and NGC generated transgenic founders; HAL assisted with data interpretation, and AVS performed statistical analyses.

**Academic Editor:** Adriano Aguzzi, Zürich University, Switzerland

**Citation:** Jankowsky JL, Slunt HH, Gonzales V, Savonenko AV, Wen JC, et al. (2005) Persistent amyloidosis following suppression of A $\beta$  production in a transgenic model of Alzheimer disease. *PLoS Med* 2(12): e355.

**Received:** June 14, 2005

**Accepted:** August 22, 2005

**Published:** November 15, 2005

**DOI:**

10.1371/journal.pmed.0020355

**Copyright:** © 2005 Jankowsky et al. This is an open-access article distributed under the terms of the Creative Commons Attribution License, which permits unrestricted use, distribution, and reproduction in any medium, provided the original author and source are credited.

**Abbreviations:** A $\beta$ , amyloid- $\beta$ ; AD, Alzheimer disease; APLP, amyloid precursor-like protein; APP, amyloid precursor protein; CaMKII $\alpha$ , calcium-calmodulin kinase II $\alpha$ ; dox, doxycycline; FA, formic acid; GFAP, glial fibrillary acidic protein; mo/huAPP695, mouse APP with a humanized A $\beta$  domain; PBS, phosphate-buffered saline; SDS, sodium dodecyl sulfate; swe/ind, Swedish/Indiana; tTA, tetracycline transactivator

\*To whom correspondence should be addressed. E-mail: jj2@caltech.edu (JJ); borchelt@mbi.ufl.edu (DRB)

‡ Current address: Department of Neuroscience, McKnight Brain Institute, University of Florida, Gainesville, Florida, United States of America

## ABSTRACT

### Background

The proteases (secretases) that cleave amyloid- $\beta$  (A $\beta$ ) peptide from the amyloid precursor protein (APP) have been the focus of considerable investigation in the development of treatments for Alzheimer disease. The prediction has been that reducing A $\beta$  production in the brain, even after the onset of clinical symptoms and the development of associated pathology, will facilitate the repair of damaged tissue and removal of amyloid lesions. However, no long-term studies using animal models of amyloid pathology have yet been performed to test this hypothesis.

### Methods and Findings

We have generated a transgenic mouse model that genetically mimics the arrest of A $\beta$  production expected from treatment with secretase inhibitors. These mice overexpress mutant APP from a vector that can be regulated by doxycycline. Under normal conditions, high-level expression of APP quickly induces fulminant amyloid pathology. We show that doxycycline administration inhibits transgenic APP expression by greater than 95% and reduces A $\beta$  production to levels found in nontransgenic mice. Suppression of transgenic A $\beta$  synthesis in this model abruptly halts the progression of amyloid pathology. However, formation and disaggregation of amyloid deposits appear to be in disequilibrium as the plaques require far longer to disperse than to assemble. Mice in which APP synthesis was suppressed for as long as 6 mo after the formation of A $\beta$  deposits retain a considerable amyloid load, with little sign of active clearance.

### Conclusion

This study demonstrates that amyloid lesions in transgenic mice are highly stable structures in vivo that are slow to disaggregate. Our findings suggest that arresting A $\beta$  production in patients with Alzheimer disease should halt the progression of pathology, but that early treatment may be imperative, as it appears that amyloid deposits, once formed, will require additional intervention to clear.

## Introduction

Over a decade ago the amyloid cascade hypothesis predicted that increased levels of amyloid- $\beta$  (A $\beta$ ) peptide lead to secondary pathologies that ultimately culminate in the onset of Alzheimer disease (AD) [1]. Early support for this hypothesis came from genetic studies linking early-onset AD to mutations in the amyloid precursor protein (APP), from which A $\beta$  is derived, and presenilins 1 and 2, which are interchangeable components of a endoprotease complex that releases A $\beta$  from APP (for review see [2,3]). If, as predicted, overproduction of A $\beta$  initiates the cascade of events leading to disease, then therapeutic strategies that lower A $\beta$  levels should either arrest or reverse the progression from peptide to dementia.

Early evidence from clinical trials of antibody-mediated clearance, one of the first A $\beta$ -lowering approaches tested in humans, suggested that treatments designed to reduce amyloid burden may indeed be beneficial. Although the trials were halted because of adverse effects in a subset of volunteers [4,5], further analysis of several patients found evidence that amyloid pathology, and to a lesser degree cognitive function, was improved in proportion to the patient's titer of A $\beta$ -specific antibody [6,7]. While this approach is promising, constant exposure to antibodies that recognize an epitope highly enriched in the brain may have unexpected side effects that will limit its long-term use.

An alternative approach that is being actively pursued for future treatment of AD seeks to lower A $\beta$  levels by limiting its production from the precursor protein APP. Peptide A $\beta$  is released from APP by the action of two enzymes, the  $\beta$ -APP cleaving enzyme 1 (BACE1) and  $\gamma$ -secretase, which cleave the holoprotein at the N- and C-termini of A $\beta$ , respectively. Several inhibitors of  $\gamma$ -secretase have already been produced [8,9], and small molecule inhibitors of  $\beta$ -APP cleaving enzyme 1 are currently being developed [10,11]. The long-term effectiveness of this approach in either humans or model systems, however, has not been reported. Although loss of  $\beta$ -APP cleaving enzyme 1 function can prevent the development of plaques in transgenic mouse models for AD (F. Laird, H. Cai, P. C. Wong, personal communication), it is not known whether the brain can clear pre-existing amyloid deposits once production of A $\beta$  has been suppressed.

Clearly, the amyloid-lowering approach should be rigorously examined in animal models before these reagents are tested in patients. However, the chemical secretase inhibitors most likely to reach human trials are still in development. Therefore, we developed a mouse model of Alzheimer-type amyloid that expresses a controllable APP transgene. This system, commonly known as the tet-off system, can be regulated by analogs of tetracycline administered in food or water [12,13]. The strong expression levels produced with the tet-off vectors, combined with the ability to reduce this expression by several orders of magnitude with tetracycline [14], allowed for a stringent test of how a highly effective pharmaceutical inhibitor of A $\beta$  production would impact the progression of amyloid pathology and whether reversal of these lesions might be possible following such treatment.

## Methods

### Transgene Construction

We created a tetracycline-responsive chimeric mouse/human APP695Swedish/Indiana (swe/ind) vector by replacing the promoter region of the moPrP.XhoI vector (also known as pPrPpE1/E2,3sal [15]) with the tetracycline-responsive promoter of pTetSplice (Life Technologies, Rockville, Maryland, United States), and then ligating mouse APP with a humanized A $\beta$  domain (mo/huAPP695) cDNA into the new vector. We began by cloning the tetracycline-responsive promoter (bp 6–481) from pTetSplice by PCR using primers that added external BamHI and NotI sites to the 5' end and a BamHI site to the 3' end, while destroying XhoI and BamHI sites within the promoter (forward: GCC GGA TCC GCG GCC GCC GTC GAG TTT ACC ACT CCC TAT C; reverse: GCC GGA TCC ACT CTA GAA GAT CCC CGG GTA CCG). We then isolated the moPrP.XhoI intron by amplification with primers that added an external BamHI site to the 5' end of exon 1 and ran through the Asp718 site of exon 2 (forward: GCC GGA TCC GAT CAG CAG ACC GAT TCT GG; reverse: GCC GGT ACC ACT AGG AAG GCA GAA TGC). This 2-kb intron fragment was cloned into a TA cloning vector (Invitrogen, Carlsbad, California, United States), then excised by Asp718 digestion and ligated to the 6.8-kb Asp718 fragment of moPrP.XhoI containing exon 2, exon 3, the 3' UTR, and pBluescript to generate an intermediate vector with all three exons and a central intron but no promoter. This vector was then opened at the BamHI site introduced by the intron cloning primer, and ligated to the 0.5-kb BamHI-cut tetracycline promoter fragment. This ligation generated a 9.3-kb vector encoding the tetracycline promoter from pTetSplice with two exons, one intron, and the original 3' UTR of the moPrP.XhoI vector, all carried in the pBluescript cloning vector.

We incorporated the Swedish (KM570/571NL) and Indiana (V617F) mutations into the mo/huAPP695 cDNA (in BS-KS) by PCR using a four-primer strategy: first, two partially overlapping products were generated in separate reactions using primers that encode the desired mutations (Swedish forward: GGA GAT CTC TGA AGT GAA TCT GGA TGC AGA ATT CCG/Indiana reverse: GGG TGA TGA AAA TCA CGG TTG C; Indiana forward: CAA CCG TGA TTT TCA TCA CCC TGG/M13 reverse). The two PCR products were ligated, digested with BglII and ApaI and cloned back into the original mo/huAPP695-BS-KS vector. Finally, the new APP695swe/ind was subcloned into the XhoI site of the moPrP-tetP vector from above to complete the construct.

### Pronuclear Injection, Screening of Founders, and Maintenance of the Lines

The moPrP-tetP-mo/huAPP695swe/ind vector was linearized and the pBluescript domain excised by digestion with NotI. The purified vector was injected into the pronucleus of fertilized eggs from C57BL/6J  $\times$  C3HeJ F1 matings. Founder animals were screened for the presence of the transgene by three-way PCR using the S36 and PrP-S/PrP-AS primers described below. Transgene-positive founders were bred to animals expressing the tetracycline transactivator (tTA) under control of the calcium-calmodulin kinase II $\alpha$  (CaMKII $\alpha$ ) promoter obtained from Jackson Laboratory [16]

(Bar Harbor, Maine, United States; stock # 3010; B6;CBA-TgN[Camk2a-tTA]1Mmay). The colony was thereafter maintained by crossing single transgenic tTA and APP offspring for each of the four APP lines. All mice were provided fresh food and water ad libitum. Animal protocols were approved by both the Johns Hopkins University and the California Institute of Technology Institutional Animal Care and Use Committees.

### Doxycycline Administration

Doxycycline (dox) was administered through commercially available dox-containing chow (BioServ, Frenchtown, New Jersey, United States). The chow contained 200 mg/kg of antibiotic; based on estimated consumption of 5 g per mouse per day, the expected dose to each animal was 1 mg dox per day. The average 25-g animal therefore received 40 µg of dox per gram body weight per day. Chow was changed 1–2 times per week to prevent breakdown of the antibiotic.

### Genotyping

Offspring were genotyped for the presence of each transgene by PCR amplification of genomic DNA extracted from a 5-mm tail biopsy. Tails were heated to 95 °C for 45 min in 250 µl of 50 mM NaOH, vortexed, then neutralized with an equal volume of 0.5 M Tris-HCl (pH 5.5). Debris was sedimented by centrifugation, and 3 µl of supernatant was used for amplification.

Genotyping for APP and tTA transgenes was performed in the same PCR reaction, using five separate primers. APP was amplified using forward primer S36 located in the 3' end of the APP cDNA (CCG AGA TCT CTG AAG TGA AGA TGG ATG) and reverse primer PrP-AS-J located in the 3' UTR of the vector (CCA AGC CTA GAC CAC GAG AAT GC). The tTA transgene was detected using a primer set that amplified across its two subdomains with tet forward located within the Tn10 tetracycline repressor (CGC TGT GGG GCA TTT TAC TTT AG) and tet reverse within the HSV1 VP16 (CAT GTC CAG ATC GAA ATC GTC). All reactions, whether transgene-positive or not, amplified a segment of the endogenous prion protein gene as a control for DNA quality using a forward primer, PrP-S-J, specific to the mouse PrP open reading frame (GGG ACT ATG TGG ACT GAT GTC GG) and a reverse primer, PrP-AS-J, shared by the 3' UTR of the endogenous PrP gene and the transgene vector. Amplification reactions were run for 37 cycles at 94 °C for 30 s, 64 °C for 1 min, and 72 °C for 1 min. All samples, transgenic and wild-type, gave a 750-bp product from the endogenous PrP gene. The APP transgene yielded an additional band at 400 bp; the tTA product fell in between at 480 bp.

### Immunoblotting/Quantitation

Frozen cortical or whole forebrain tissue was homogenized by sonication in five volumes of phosphate-buffered saline (PBS) with 5 mM EDTA and protease inhibitors (Mammalian cell cocktail, Sigma, St. Louis, Missouri, United States), using a probe sonicator set to 50% output (TEKMAR, Cincinnati, Ohio, United States). After dilution with an equal volume of PBS/EDTA/protease inhibitor, the samples were centrifuged briefly and the supernatant used for analysis. Fifty micrograms (6E10 and CT15) or 5 µg (22C11) of brain homogenate was loaded per lane onto 7.5%, 10%–20%, or 4%–20% Tris-HCl PAGE gels (Bio-Rad Laboratories, Hercules, California,

United States) and electrophoresed for several hours in 1× Tris-glycine-sodium dodecyl sulfate (1×TG-SDS) buffer (6E10 and 22C11; Amresco, Solon, Ohio, United States) or 1× Tris-tricine-SDS buffer (CT15; Invitrogen, Carlsbad, California, United States). Proteins were transferred overnight to 0.45-µm Optitran nitrocellulose (Schleicher and Schuell, Keene, New Hampshire, United States) in 1× TG buffer (Amresco). Blots were blocked in PBS containing 5% nonfat dry milk powder, and incubated for 3 h at room temperature in blocking solution with one of the following antibodies: mouse monoclonal 22C11 (kind gift of Konrad Beyreuther and Andreas Weidemann; [17]) diluted 1:1,000, mouse monoclonal 6E10 (Signet Laboratories, Dedham, Massachusetts, United States) diluted 1:2,500, rabbit polyclonal anti-superoxide dismutase 1 (m/hSOD1) [18] diluted 1:2,500 to 1:4,000, or rabbit polyclonal CT15 (kind gift of Ed Koo; [19]) diluted 1:1,000. Subsequently, the blots were washed with PBS containing 0.1% Tween-20, and then incubated with either goat anti-mouse- or goat anti-rabbit-HRP conjugated secondary antibody diluted 1:1,000 in blocking solution. After several additional rinses in PBS with 0.1% Tween-20, blots were developed with enhanced chemiluminescence reagent and imaged with the Bio-Rad Molecular Imager FX system.

Staining intensity within each lane was quantified using the Quantity One image analysis software (Molecular Imager FX, Bio-Rad Laboratories). Background was calculated from across the image and subtracted from the entire file. The signal intensity for each band (corrected signal intensity × pixel number) was then calculated using the Volume report tool.

### Slot Blot mRNA Analysis

Five micrograms per sample of total RNA extracted from fresh-frozen brain, liver, kidney, heart, lung, spleen, and skeletal muscle was vacuum-filtered through 0.45-µm Optitran nitrocellulose. After several washes through the manifold with 10× SSC, blots were UV-cross-linked and probed with a radiolabeled ~350-bp BglIII-XhoI cDNA fragment of mol/huAPP695 cDNA. After hybridizing overnight at 65 °C in 1% BSA/1 mM EDTA/0.5 M sodium phosphate buffer (pH 7.2)/7% SDS [20], the blots were washed twice at 65 °C for 30 min each in 0.1% BSA/1 mM EDTA/40 mM sodium phosphate buffer (pH 7.2)/5% SDS before two final 30-min washes at 65 °C with 1 mM EDTA/40 mM sodium phosphate buffer (pH 7.2)/1% SDS. Blots were wrapped wet and exposed to phosphorscreens overnight at room temperature.

### Amyloid Histology

Mice were euthanized by ether inhalation and brains removed for immersion fixation in 4% paraformaldehyde/1× PBS. After 48 h in fixative at 4 °C, brains were transferred to PBS, dehydrated in alcohols, treated with cedarwood oil and methylsalicylate, and embedded in paraffin for sectioning.

**Hirano silver stain.** Silver impregnation histology was performed on 10-µm paraffin-embedded sections by Hirano's modification of the Bielschowsky method [21]. Briefly, sections were deparaffinized through xylene and alcohols into tap water before being placed into fresh 20% silver nitrate solution for 20 min. After being washed thoroughly with distilled water, slides were immersed in 20% silver nitrate solution titrated with fresh ammonium hydroxide.

After 20 min, slides were washed with ammonia water before being individually developed with 100  $\mu$ l of developer (20 ml of 37% formaldehyde, 100 ml of distilled water, 50  $\mu$ l of concentrated nitric acid, and 0.5 g of citric acid) added to 50 ml of titrated silver nitrate solution. Slides were then rinsed in tap water, fixed in 5% sodium thiosulfate, and dehydrated through alcohols and xylene.

**Thioflavin-S staining.** Following deparaffinization of sections through xylene and alcohols, amyloid impregnation with thioflavin-S was performed according to the Guntern modification of the standard protocol. Slides holding 10- $\mu$ m paraffin sections were washed twice in distilled water, then immersed for 5 min in a 0.25% potassium permanganate solution, followed by 5 min in a 1% potassium metabisulfate/1% oxalic acid solution. After this preparation, slides were placed into a filtered aqueous 0.02% thioflavin-S solution (Chroma-Gesellschaft Schmid, Kongen, Germany) for 8 min. Excess stain was removed by two brief rinses in 80% ethanol, then two in distilled water, after which slides were finished in aqueous mounting medium for fluorescence photomicrography.

**Ubiquitin, glial fibrillary acidic protein, and A $\beta$  immunohistochemistry.** Prior to immunostaining, slides were deparaffinized by oven heating followed by immersion in xylene. After rehydration through graded alcohols into tap water, endogenous peroxidase activity was quenched by incubation with 3% hydrogen peroxide in methanol. Slides were microwaved for 5–7 min in water, cooled for 5 min, then washed in TBS. Nonspecific staining was blocked for 1 h with 3% normal goat serum and 0.1% Triton-X 100 in TBS. Slides were then placed into primary antibody (rabbit anti-A $\beta$  peptide polyclonal antibody, Zymed Laboratories, South San Francisco, California, United States; rabbit anti-ubiquitin and rabbit anti-glial fibrillary acidic protein (GFAP) polyclonal antibodies, Dako, Carpinteria, California, United States) diluted 1:500 in TBS with 2% normal goat serum and incubated overnight at room temperature. After being washed of excess primary antibody with several changes of TBS, slides were incubated with either the Vectastain Elite anti-rabbit secondary system (anti-A $\beta$ ; Vector Laboratories, Burlingame, California, United States) or peroxidase/anti-peroxidase reagents (anti-ubiquitin and anti-GFAP; Sternberger Monoclonals, Lutherville, Maryland, United States) according to the manufacturers' directions. Antibody binding was visualized with diaminobenzidine, and sections were counterstained with hematoxylin.

### Filter Trap Assay

An aliquot of each cortical homogenate used for Western blotting above was partially solubilized by the addition of SDS to a final concentration of 1%. Serial 1:2 dilutions were made with 1 $\times$  PBS/1% SDS, and 100  $\mu$ l of each dilution was then vacuum-filtered through a pre-wet 0.22- $\mu$ m cellulose acetate membrane (Schleicher and Schuell) [22]. Each well was washed several times with PBS, after which blots were incubated overnight with polyclonal anti-A $\beta$  antibody (Zymed Laboratories) diluted 1:600 in a blocking solution of 1 $\times$  TBS/5% nonfat dry milk powder. After washing the blots three times for 10 min each in 1 $\times$  TBS/0.1% Tween-20, the membrane was incubated for 1 h with HRP-conjugated protein A (Sigma) diluted 1:5,000 in blocking solution. The membranes were again washed three times with 1 $\times$  TBS/0.1%

Tween-20, before antibody binding was detected with enhanced chemiluminescence (PerkinElmer, Boston, Massachusetts, United States). Digital images of each blot were captured with a Molecular Imager FX gel documentation system, and the intensity of A $\beta$  staining was quantified using Quantity One image analysis software.

### A $\beta$ ELISA

An aliquot of cortical homogenate generated for Western analysis described above was subjected to a three-step sequential extraction using PBS, 2% SDS, and 70% formic acid (FA). At each step, the sample was sonicated in appropriate buffer and centrifuged at 100,000g for 30 min (1- to 1.5-mo samples) or 60 min (6- to 12-mo samples) at 4  $^{\circ}$ C as previously described [23–25]. The supernatant was removed for analysis, and the pellet was sonicated in the next solution in sequence. The 2% SDS extracts were diluted in EC buffer, and the FA extracts neutralized with 1M Tris-phosphate buffer (pH 11) then diluted with EC buffer prior to testing. Human A $\beta$  was measured in each fraction using BAN50 for capture (epitope A $\beta$ 1–16) and BA27 and BC05 for detection (A $\beta$ 40 and A $\beta$ 42, respectively) (Takeda Chemical Industries, Osaka, Japan). Total A $\beta$  (mouse + human; 1- to 1.5-mo samples only) was measured in each fraction using BNT77 for capture (epitope A $\beta$ 11–28) and BA27 and BC05 for detection. All values were calculated as picomoles per gram based on the initial weight of cortical tissue.

### Activity Monitoring

Daily basal activity was studied in 28 CaMKII $\alpha$ -tTA  $\times$  tet-APPsw/ind line 107 mice between 4 and 5 mo of age. Animals were separated into individual cages immediately before the start of each experiment ( $n = 3$ –6 per genotype untreated, 2–5 per genotype dox-reared). The cages were placed inside activity-monitoring frames designed to count every time the animal passed through one of three photobeams spanning the width of the cage (San Diego Instruments, San Diego, California, United States). Experiments were started midway through the light phase of the day, and data were collected in 1-h bins for the following 48 h. Testing rooms were maintained on the same 13:11 h day:night cycle as the main animal housing areas and were closed to entry during the experiment.

### Statistical Analyses

Statistical analyses of protein expression, ELISA data, and filter trap assays were performed by ANOVA with Tukey's honest significant difference post-hoc test applied to significant main effects or interactions (Statistica 6.0, StatSoft, Tulsa, Oklahoma, United States). In cases of positively skewed data distribution,  $\log_{10}(x + 0.5)$  transformation was applied to the raw data before submitting them to ANOVA.

### Results

We used the tet-off transgene system to express a double mutant version of chimeric mo/huAPP695 (swe/ind KM570, 571NL, and V617F) from a tetracycline-responsive promoter [12,13]. Transgenic APP expression was activated by crossing the APPsw/ind mice to animals producing tTA under control of the CaMKII $\alpha$  promoter [16]. After initial screening of



founders, we identified four lines of tet-APP<sup>swe/ind</sup> mice that produced very high levels of transgene product in offspring coexpressing tTA (Figures 1 and S1). Compared to a standard APP transgenic line used for previous amyloid studies by our laboratory (line C3-3; [15,26,27]), we estimated that the four controllable lines produce transgenic APP protein at 10- to 30-fold over endogenous levels (Figure S1). This estimate was confirmed by direct comparison of APP levels in non-transgenic and tet-off APP mice using an antibody that recognizes both endogenous APP (and amyloid precursor-like protein 2) and the transgenic protein (monoclonal antibody 22C11; Figure 1D).

Importantly, all four new lines of tet-off APP mice showed nearly complete suppression of the transgene following dox treatment (Figures 1 and S1). We focused on one of the four lines, line 107, to examine in more detail the time dependence and extent of transgene suppression following either acute or chronic treatment with dox. Two dox-treated groups were compared to two untreated groups: one group of mice was born and raised on dox, a second group was treated with dox for 2 wk starting at 1 mo of age (4 wk + 2 wk dox); two untreated groups kept on normal chow were harvested at either 4 or 6 wk of age. Animals born and raised on dox

harbored no transgenic APP (Figure 1A). Following as little as 2 wk of dox treatment, transgenic APP expression was reduced by more than 95% compared to pre-dox levels. The residual expression remaining in acutely treated mice represents less than 4% of the transgenic protein produced in the absence of dox (Figure 1C), and likely results from slight leakage at the level of transcription (data not shown). Importantly, the total amount of APP (endogenous plus transgenic) and related APLPs in both acute and chronically treated animals was statistically indistinguishable from that in nontransgenic mice (Figure 1D; statistical analyses for experiments throughout the study are presented in the accompanying figure legends).

To ensure that A $\beta$  production was suppressed in concert with the dox-mediated inhibition of its precursor APP<sup>swe/ind</sup>, we measured A $\beta$ 40 and A $\beta$ 42 levels by ELISA in forebrain homogenates from young tet-off animals. At 1 mo of age, the mice lacked visible amyloid aggregates that might act as an intractable reservoir of peptide remaining in the brain after the transgene had been suppressed. To further ensure we could detect any such insoluble aggregates that might bias our measure of changes in peptide synthesis, we performed a sequential three-step extraction with PBS, 2% SDS, and 70%

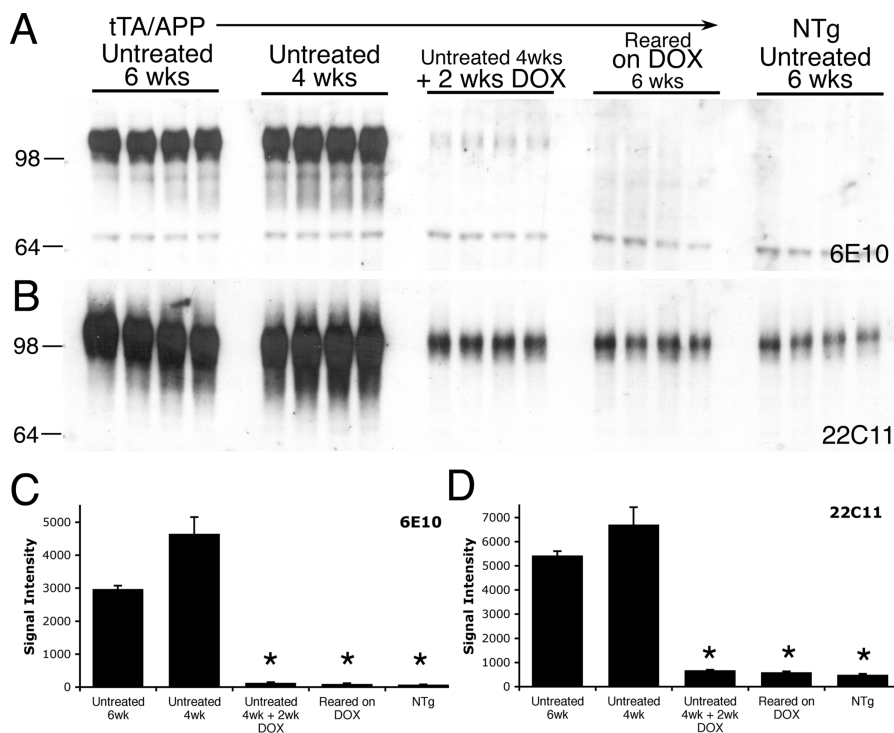


**Figure 1. Control of Transgenic APP Expression by Dox**

(A) Western blotting for transgenic APP using the human-specific 6E10 antibody shows expression of full-length protein in forebrain tissue from young predeposit double transgenic animals (line 107) and its suppression following dox treatment. Untreated animals show high levels of transgene expression; protein levels drop dramatically in animals acutely treated with dox for 2 wk. A faint, but detectable band of full-length protein remains in acutely treated animals that can be eliminated in mice born and raised on dox.

(B) Immunoblotting with the N-terminal antibody 22C11 to detect both transgenic and endogenous protein shows that dox treatment reduces APP/APLP to levels found in nontransgenic mice.

(C) Measurement of signal intensity from the Western blot in (A) shows transgenic APP levels are decreased more than 95% by dox in both acutely and chronically treated animals (97.2% for 4 wk + 2 wk dox, 98.0% for reared on dox versus 4 wk untreated; ANOVA effect of treatment group  $F_{4,15} = 85.55$ ,  $p < 0.001$ ). APP levels in 4 wk + 2 wk dox, reared on dox, and nontransgenic (NTg) were not significantly different ( $p > 0.9$ , Tukey post-hoc test).

(D) Measurement of signal intensity from the Western blot in (B) shows total APP/APLP levels in dox-treated tTA/APP mice are significantly lower than in 4-wk-old untreated mice (ANOVA effect of treatment group  $F_{4,15} = 84.41$ ,  $p < 0.001$ ) and indistinguishable from those of nontransgenic animals ( $p > 0.9$ , Tukey post-hoc test). \*,  $p < 0.001$  versus untreated 4-wk-old mice, Tukey post-hoc test applied to significant effect of group ANOVA.

DOI: 10.1371/journal.pmed.0020355.g001

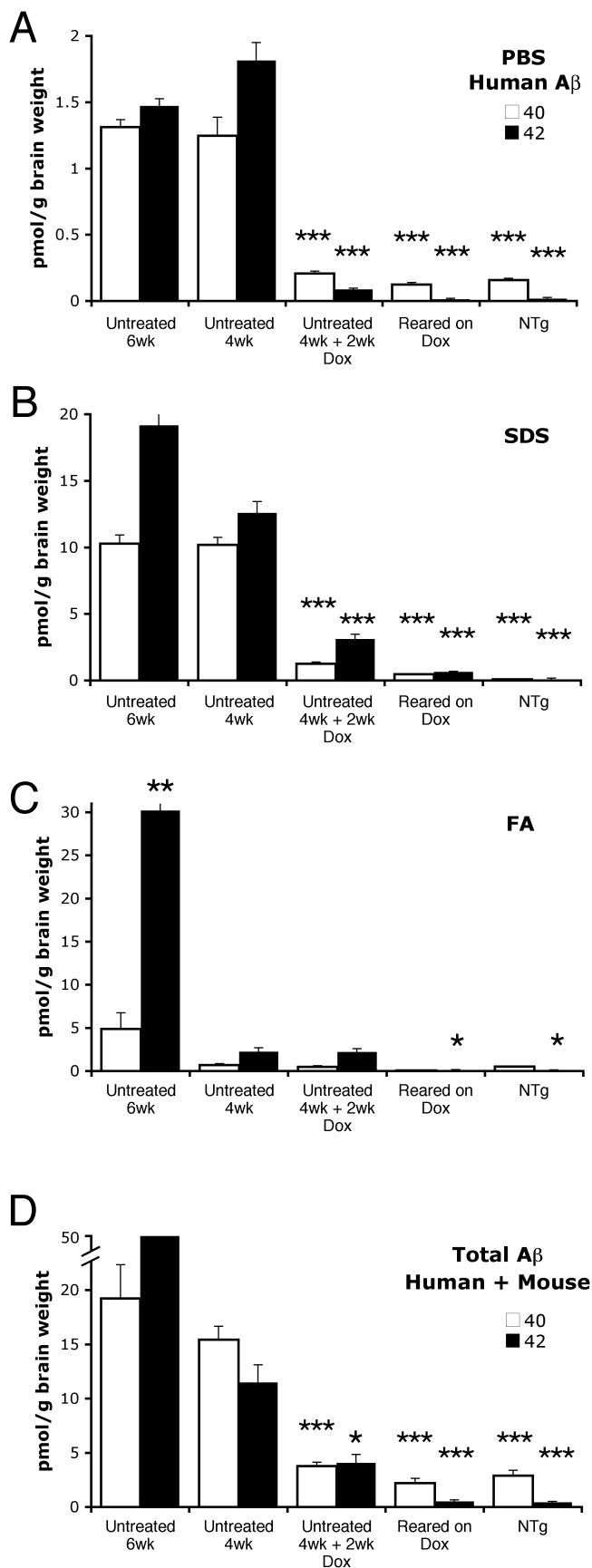


**Figure 2.** Aβ Levels Are Dramatically Reduced by Transgene Suppression

Cortical homogenates from young, predeposited tTA/APP mice used for Western blot in Figure 1 (line 107) were fractionated by sequential multi-step extraction with PBS, 2% SDS, and 70% FA followed by human-specific Aβ ELISA to measure transgene-derived peptide in each fraction. Aβ40 is shown in white, Aβ42 in black.

(A) PBS-soluble Aβ levels are substantially reduced by both acute and chronic dox treatment (ANOVA, effect of treatment group  $F_{4,24} = 137.10$  and  $386.01$ ,  $p < 0.001$ , for Aβ40 and Aβ42, respectively). Aβ levels in treated animals are indistinguishable from nontransgenic (NTg) animals ( $p > 0.3$ , Tukey post-hoc test).

(B) In the young animals tested here prior to the formation of visible amyloid deposits, most Aβ is extracted into the SDS fraction (84% and 76% of all transgene-derived Aβ40 and Aβ42, respectively). As in the PBS-soluble fraction, Aβ levels in the SDS fraction are significantly lowered by dox treatment compared to untreated animals (ANOVA effect of group  $F_{4,24} = 197.57$  and  $163.48$ ,  $p < 0.001$ , for Aβ40 and Aβ42, respectively). Acutely treated animals retained a small (although significant) amount of residual peptide ( $p < 0.001$  compared to nontransgenic, Tukey post-hoc test), whereas Aβ levels in mice born and raised on dox were reduced to levels indistinguishable from nontransgenic ( $p > 0.8$ , Tukey post-hoc test).

(C) The FA-soluble fraction already contains a small but significant pool of aggregated Aβ42 in untreated animals by 4 wk of age ( $p < 0.05$  versus nontransgenic; Tukey post-hoc test applied to significant effect of group ANOVA  $F_{4,24} = 17.11$ ,  $p < 0.001$ ). By 6 wk of age, the amount of Aβ in the FA fraction is increased significantly preceding the appearance of visible deposits 2 wk later. The FA pool is the only peptide fraction not lowered by acute dox treatment (4 wk untreated = 4 wk + 2 wk dox,  $p > 0.9$ , Tukey post-hoc test), consistent with poor turnover of aggregated Aβ species.

(D) Measurements of total Aβ, including both endogenous and transgene-derived peptides, show that animals born and raised on dox harbor Aβ levels identical to nontransgenic animals ( $p > 0.9$ , Tukey post-hoc test, effect of group ANOVA  $F_{4,24} = 39.13$  and  $35.29$ ,  $p < 0.001$ , for Aβ40 and Aβ42, respectively). Whereas chronic transgene suppression fully prevents synthesis of both peptides, acute dox treatment fully suppresses Aβ40 levels ( $p > 0.8$ , Tukey post-hoc test), but leaves a small amount of nonsuppressed Aβ42. The residual Aβ42 observed in acutely treated young animals derives from uncleared aggregates extracted in the SDS and FA fractions. \*,  $p < 0.05$ ; \*\*,  $p < 0.005$ ; \*\*\*,  $p < 0.001$  versus 4-wk-old untreated mice, Tukey post-hoc applied to significant effect of group ANOVA.

DOI: 10.1371/journal.pmed.0020355.g002

FA that would separate peptides by solubility. We compared the levels of human transgene-derived Aβ40 and Aβ42 in untreated mice at 4 and 6 wk of age to animals that had either been born and raised on dox or that had been left untreated for 4 wk and then placed on dox chow for 2 wk prior to harvest (the same groups described above for immunoblot analysis of APP<sup>swe/ind</sup> levels, line 107). Consistent with the reduction in full-length APP<sup>swe/ind</sup> synthesis shown by immunoblot (see Figure 1), we found that transgene-derived Aβ levels were completely suppressed in animals born and raised on dox, and were sharply reduced following acute (2 wk) antibiotic treatment. Compared to the levels in untreated 4-wk-old mice, PBS-soluble Aβ42 dropped by 95.2% following 2 wk of dox treatment and by 99.2% with chronic treatment (Figure 2A). Similarly, SDS-soluble Aβ42 decreased by 75.2% and 94.8% following 2-wk or lifelong dox treatment (Figure 2B). Only the FA fraction revealed a small dox-resistant pool of peptide in acutely treated animals that we believe represents stable predeposited aggregates that have already accumulated by 4 wk of age when treatment was begun (Figure 2C). Indeed, animals that were born and raised on dox did not harbor this reservoir of treatment-resistant peptide, with 96.3% less Aβ42 than untreated 4-wk-old mice. Measurement of total Aβ in chronically treated mice, including endogenous and transgene-derived peptide, demonstrated that Aβ levels in tet-off APP mice were reduced to the level of

endogenous peptide found in nontransgenic animals (Figure 2D). Taken together with the immunoblotting data for full-length APP<sub>swE/ind</sub>, the ELISA measurements indicate that dox-mediated suppression of transgenic APP<sub>swE/ind</sub> synthesis leads to parallel reduction of A $\beta$  levels.

The ELISA data also confirmed that incorporation of the Swedish and Indiana mutations led to high levels of A $\beta$ 42, which we predicted would induce rapid plaque formation in untreated animals. Histological characterization of double transgenic (CaMKII $\alpha$ -tTA  $\times$  tet-APP<sub>swE/ind</sub>) mice revealed early-onset amyloid formation in all four new lines. Amyloid plaques were seen in mice as young as 8 wk of age (data not shown). Plaques were limited to the forebrain, including the cortex, hippocampus, olfactory bulb, and striatum, where the CaMKII $\alpha$  promoter is known to be most active [16,28] (Figure S2). By 6 mo of age, amyloid burden became severe, covering large areas of the cortex and hippocampus (Figure S3). No lesions were seen in the cerebellum or brain stem even at late ages, consistent with CaMKII $\alpha$ -controlled transgene expression. Unlike what is thought to occur in the human disease, the first visible plaques in the tet-off APP mice are fibrillar-cored deposits. We have noted the same early appearance of cored deposits in other lines of APP transgenic mice that harbor the Swedish mutation [27]. Diffuse plaques were apparent in 6-mo-old tTA/APP mice, and became relatively abundant by 9 mo of age. At older ages (9–12 mo) amyloid deposits were visible in the thalamus, which has also been observed in mice expressing mutant APP via the Thy-1 promoter. The presence of amyloid pathology in this region has been attributed to axonal transport of APP/A $\beta$  to the terminals of cortical neurons in the thalamus [29]. Most importantly, only double transgenic mice, expressing both the tTA and APP transgenes, developed amyloid lesions. Single transgenic mice up to 15 mo of age showed no sign of pathology (Figure S3). Similarly, amyloid pathology can be completely prevented in double transgenic animals born and raised on dox. Animals from our highest expressing line (line 885) maintained on dox for up to 1 y harbored no amyloid pathology (data not shown), indicating that residual leakage of transgene expression in the presence of dox does not provide sufficient A $\beta$  peptide to induce amyloid formation even over long periods.

To mimic therapeutic intervention with inhibitors of A $\beta$  production, we raised a group of 25 double transgenic mice (CaMKII $\alpha$ -tTA  $\times$  APP line 107) on normal food until 6 mo of age, when we knew amyloid formation was already well underway in the brain. At 6 mo, half of the animals were switched from normal chow to food containing dox at 200 mg/kg until they were sacrificed at 9 or 12 mo of age. The remaining control animals were kept on standard chow (untreated). In all, four cohorts were created: 6 mo untreated ( $n = 7$ ), 9 mo untreated ( $n = 5$ ), 6 mo + 3 mo treated ( $n = 8$ ), and 6 mo + 6 mo treated ( $n = 5$ ). Full suppression (>95%) of transgenic APP<sub>swE/ind</sub> levels in the dox-treated animals was confirmed by immunoblot (Figure 3). To ensure that the transgene could be suppressed as rapidly in 6-mo-old mice with fulminant pathology as it can in young, predeposit animals, we treated an additional set of 6-mo-old animals with dox for 1 wk prior to harvest. Importantly, both APP<sub>swE/ind</sub> and APP-C-terminal fragment levels were fully suppressed after only 1 wk of treatment, indicating that the in

vivo half-life of APP<sub>swE/ind</sub> and its processed C-terminal fragments are relatively short (Figure 3D).

Tissue sections from each animal in the four treatment groups were stained for amyloid pathology by Hirano silver, Campbell-Switzer silver, thioflavin-S, and A $\beta$  immunohistochemistry. As expected, the 6 mo untreated cohort displayed moderate amyloid pathology, and the 9 mo untreated cohort progressed to a severe amyloid burden. In contrast, the extent of amyloid pathology in mice from the 6 mo + 3 mo treated or 6 mo + 6 mo treated cohorts closely resembled that of the 6 mo untreated cohort, despite the significant age difference between the treated and untreated groups (Figures 4 and S3). Well-formed plaques remained in the treated animals after 6 mo of transgene suppression, even though as much time was given to clear the lesions as they had taken to form. Moreover, both types of amyloid, diffuse and fibrillar, remained intact throughout treatment. Using the Campbell-Switzer silver stain to distinguish different forms of amyloid, we found diffuse plaques were as persistent as cored deposits (Figure S4). It was nevertheless clear that dox-induced suppression of transgenic APP had completely halted the progression of pathology.

To confirm that the arrest of plaques without any sign of clearance was not unique to the line 107 mice, we repeated the dox-suppression experiment in a second line of tet-off APP mice (CaMKII $\alpha$ -tTA  $\times$  tet-APP<sub>swE/ind</sub> line 18;  $n = 22$ ). Again, long-term dox treatment was begun at 6 mo of age, and mice were harvested after 3 mo of transgene suppression (6 mo untreated,  $n = 8$ ; 9 mo untreated,  $n = 6$ ; 6 mo + 3 mo treated,  $n = 8$ ). Immunoblotting for APP confirmed full transgene suppression in the treated animals (Figure S5). As in the line 107 mice described above, amyloid burden worsened substantially in the untreated mice between 6 and 9 mo of age. Suppression of transgene expression abruptly arrested progression of pathology (Figure S6), but again without any sign of reduction. Both silver- and thioflavin-S-positive plaques could still be found in each of the dox-treated animals.

We biochemically measured the amount of aggregated A $\beta$  in the brains of our mice before and after transgene suppression using filter trap analysis of cortical tissue from each animal. In this assay, serial dilutions of protein homogenate are passed through a cellulose acetate filter; particles larger than the pore size of the filter become trapped in the membrane and are revealed by immunoblotting [22]. Consistent with our visual analysis of the histological sections, line 107 tTA/APP mice treated with dox for 3 or 6 mo had the same amount of aggregated A $\beta$  as when they started treatment at 6 mo of age (Figure 4A and 4B). In contrast, untreated 9-mo-old mice had almost twice as much aggregated A $\beta$  as either of the treated groups. Filter trap analysis of line 18 tTA/APP mice yielded similar results: the increase in aggregated A $\beta$  observed in untreated animals between 6 and 9 mo of age was completely arrested by transgene suppression (Figure S5C and S5D).

We next used ELISA to measure total A $\beta$  in the brains of each group to determine whether any change in the amount or solubility of peptide occurred while APP<sub>swE/ind</sub> expression was suppressed. Cortical homogenates were sequentially extracted to separate peptide into PBS-, SDS-, and FA-soluble fractions, then transgene-derived A $\beta$ 40 and A $\beta$ 42 were measured by human-specific ELISA [23]. In all animals

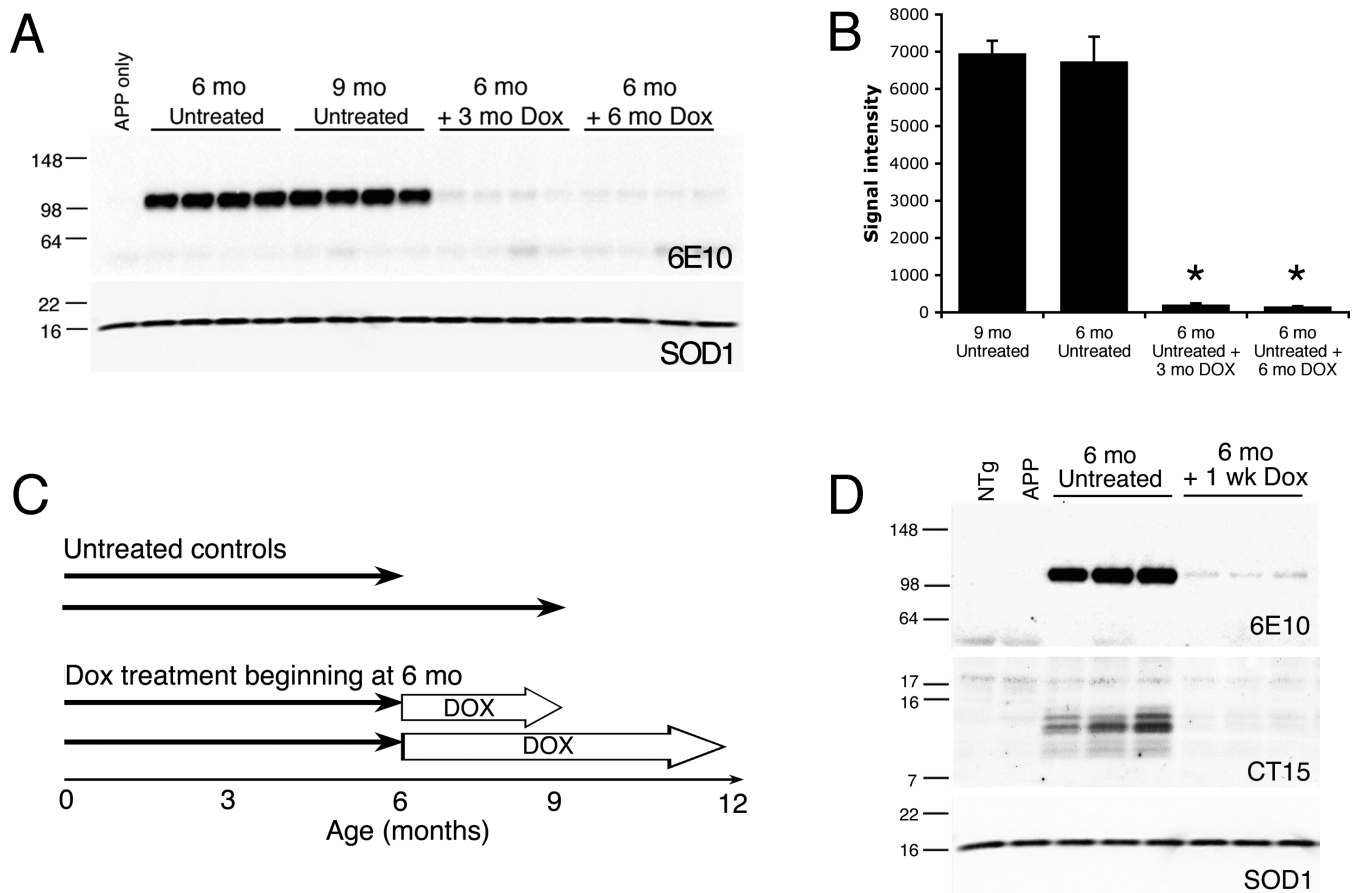


**Figure 3. Robust Transgene Suppression in Older Mice with Preexisting Amyloid Pathology**

(A) Cortical homogenates from 6- to 12-mo-old animals used for pathology studies described below (line 107) were immunoblotted with human-specific antibody 6E10 to examine transgene suppression following 3 or 6 mo of dox treatment. The blot was co-immunostained for endogenous superoxide dismutase 1 (SOD1) as a control for loading.

(B) Quantitation of signal intensity from the Western blot shown in (A). Transgenic APP levels are significantly suppressed following 3 or 6 mo of dox treatment (96.9% and 97.6%, respectively). \*,  $p < 0.001$  compared to 6-mo-old untreated animals, Tukey post-hoc test applied to significant effect of group ANOVA  $F_{3,12} = 107.22$ ,  $p < 0.001$ . These data demonstrate that strong transgene suppression is attained both before and after the onset of amyloid pathology (see Figure 1 for predeposits experiments).

(C) Experimental design. To examine the effects of chronic A $\beta$  suppression on amyloid pathology after the onset of deposition, we compared untreated controls harvested at 6 and 9 mo of age to animals placed on dox at 6 mo of age and harvested after 3 or 6 mo of treatment.

(D) Dox treatment leads to rapid transgene suppression even in 6-mo-old tTA/APP mice. Immunostaining with 6E10 shows APP<sub>swe/ind</sub> levels are dramatically reduced in 6-mo-old mice treated for 1 wk with dox (upper panel). A separate blot was immunostained for APP C-terminal fragments with CT15 antibody to show that the precursors to A $\beta$  cleavage are decreased in parallel with the full-length protein (middle panel). Costaining for superoxide dismutase 1 was used as an internal control for loading (lower panel, taken from bottom half of 6E10 blot).

DOI: 10.1371/journal.pmed.0020355.g003

harboring amyloid deposits, we found that the vast majority of A $\beta$  (>99%) was extracted into the SDS and FA fractions (Figure 5A and 5B). Consistent with the filter trap results presented above, there were no significant differences in SDS- or FA-soluble A $\beta$  between the 6 mo untreated cohort and either the 6 mo + 3 mo treated or 6 mo + 6 mo treated cohorts. However, brains of both 6 mo + 3 mo and 6 mo + 6 mo treated cohorts contained roughly twice as much PBS-soluble A $\beta$ 40 as untreated 6-mo-old mice (Figure 5C). Levels of A $\beta$ 42 showed a similar trend, but did not reach statistical significance. In fact, levels of PBS-soluble A $\beta$ 40 and A $\beta$ 42 in the 6 mo + 3 mo and 6 mo + 6 mo treated cohorts were most similar to that of the 9 mo untreated cohort, suggesting that age, as opposed to synthetic rate (which would be negligible in the treated animals), may determine the fraction of PBS-soluble A $\beta$  in these animals.

We also assessed neuritic and glial pathology surrounding the plaques to determine whether there were any changes in nearby tissue following long-term transgene suppression. Both Hirano silver stain and ubiquitin immunostaining showed neuritic pathology in all treatment groups (Figure 6). Similarly, activated astrocytes immunostained for GFAP were found near plaques in all animals (Figure 6). Neuritic and glial pathology were more severe in the older untreated mice. In contrast, transgene suppression prevented the growth of individual deposits apparent in untreated mice, and limited the surrounding pathology to what was already present when treatment began.

An obvious question we sought to address was whether the deposition of A $\beta$  diminished cognitive ability in untreated mice, and what might happen to cognition when the process was interrupted. Unfortunately, efforts to characterize



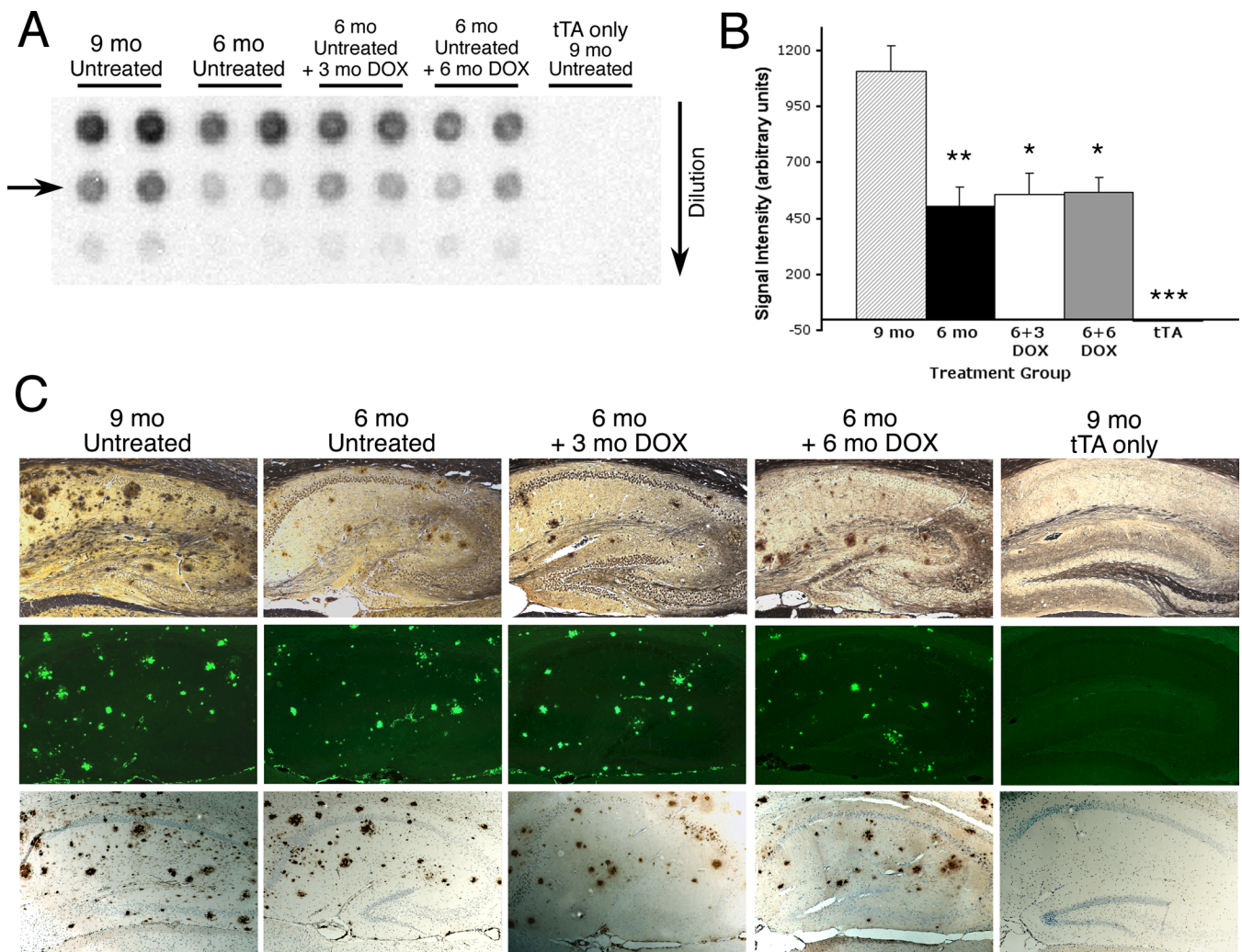


**Figure 4.** Suppression of Transgenic APP Arrests Progression of Amyloid Pathology

(A) Aggregated A $\beta$  was quantified in cortical tissue from dox-treated and control tTA/APP mice (line 107) using a filter trap assay. Serial dilutions of protein homogenate were passed through a cellulose acetate filter; protein aggregates larger than the pore size were trapped and immunostained for A $\beta$ .

(B) Quantitation of signal intensity in the linear range of each filter trap dilution series (arrow in [A]) was used to compare aggregate load across treatment groups. Aggregated A $\beta$  increased significantly between 6 and 9 mo of age in untreated mice (significant effect of group ANOVA  $F_{3,18} = 7.85$ ,  $p < 0.002$ ). This progression of pathology was completely prevented by transgene suppression. The amount of aggregated A $\beta$  was identical in untreated mice at 6 mo of age to that in 9- or 12-mo-old animals treated with dox ( $p > 0.9$ , Tukey post-hoc test). Single transgenic tTA samples were included as negative controls and showed no signal above background. \*,  $p < 0.01$ ; \*\*,  $p < 0.005$  versus 9-mo-old untreated mice, Tukey post-hoc test; \*\*\*,  $p < 0.001$  versus 9-mo-old untreated mice, Student's  $t$ -test.

(C) Amyloid pathology in the hippocampus of representative mice from each treatment group: Hirano silver stain (top row), thioflavin-S (middle row), and A $\beta$  immunohistochemistry (bottom row). Amyloid burden increases dramatically between 6 and 9 mo of age in untreated mice, but remains stable in transgene-suppressed mice over the same period (6 mo + 3 mo dox and 6 mo + 6 mo dox). Single transgenic animals (tTA only shown here) show no sign of amyloid pathology at any age tested.

DOI: 10.1371/journal.pmed.0020355.g004

cognitive behavior were compromised by severe hyperactivity in untreated double transgenic mice. The tTA/APP animals were often seen running in circles around the perimeter of their cages, and a similar swimming pattern was noted when the mice were tested in the Morris water maze. In the radial water maze, repetitive swim patterns were noted with no evidence of choice-motivated actions. Other studies have dealt with similar problems by excluding animals that do not show adequate attention to the task, retaining only those mice that meet certain performance criteria [30]. In our case, the penetrance of hyperactivity was close to 100%, leaving us with no testable animals. This phenotype has not affected

previous lines of APP<sup>sw</sup> mice we have produced, such as lines E1-2 or C3-3, that express lower levels of transgenic protein. Indeed, in past studies where hyperactivity was not a factor, we established a clear relationship between amyloid load and cognitive ability [31]. However, in the current study, we feel that although the poor performance of the tTA/APP mice in the maze tests could technically be scored as cognitive impairment, the animals' severe hyperactivity made interpretation of the cognitive tasks impossible.

In order to understand the nature and extent of hyperactivity in the tTA/APP mice, we quantified daily activity levels in double transgenic animals along with their single

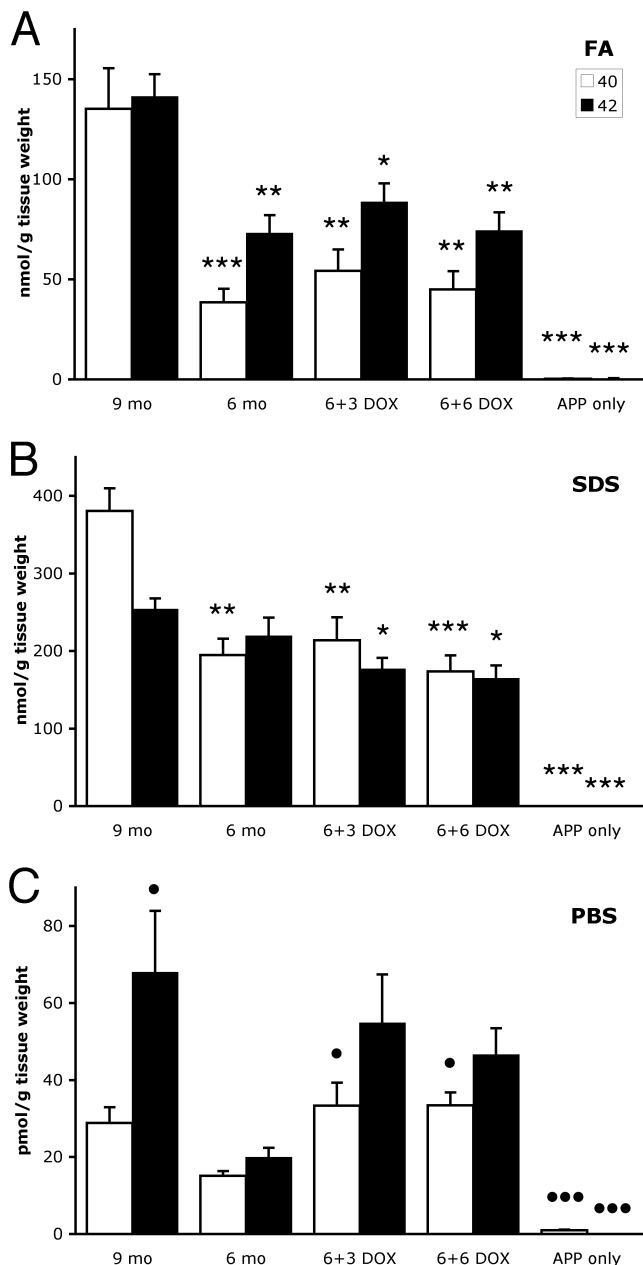


**Figure 5.** Aβ ELISA Confirms Arrest of Progression without Clearance of Peptide in Mice with Preexisting Aggregates

Aβ levels in untreated 6- and 9-mo-old tTA/APP line 107 mice (shown in Figure 4) were compared to those in 9- and 12-mo-old animals treated with dox from the age of 6 mo. Single transgenic APP samples were included as negative controls. Cortical homogenates were fractionated by sequential multi-step extraction with PBS, 2% SDS, and 70% FA followed by human-specific Aβ ELISA to measure transgene-derived peptide in each fraction. Aβ40 is shown in white, Aβ42 in black.

(A and B) Most Aβ in the brains of plaque-bearing mice is extracted into the FA and SDS fractions. Consistent with amyloid burden (Figures 4 and S3), SDS- and FA-extracted Aβ levels in untreated 9-mo-old mice were significantly higher than in untreated 6-mo-old mice (Tukey post-hoc test applied to significant effect of group ANOVA for SDS and FA fractions  $F_{3,18} = 4.72$ – $12.92$ ,  $p < 0.02$ ). In contrast, 3 or 6 mo of transgene suppression held Aβ at levels equivalent to those harbored when treatment was started ( $p > 0.2$  compared to 6 mo untreated mice, Tukey post-hoc test). \*,  $p < 0.05$ ; \*\*,  $p < 0.005$ ; \*\*\*,  $p < 0.001$  versus 9-mo-old untreated mice, Tukey post-hoc test. Significance for APP versus 9-mo-old untreated mice is based on Student's *t*-test.

(C) The PBS fraction represents less than 0.1% of total Aβ (note the change in y-axis from [A] and [B]), but only here do Aβ levels in the dox-treated mice differ from those in younger untreated mice. Although both peptides appear elevated in the treated groups compared to the untreated 6-mo-old mice, only Aβ40 reaches statistical significance ( $p < 0.05$ , Tukey post-hoc test applied to significant effect of group ANOVA for Aβ40  $F_{3,18} = 4.60$ ,  $p < 0.02$ ). A similar trend was seen for Aβ42, where ANOVA yielded a significant effect of group for PBS-soluble Aβ42 ( $F_{3,18} = 3.75$ ,  $p < 0.03$ ), however this was due only to differences between the untreated 6- and 9-mo-old groups. •,  $p < 0.05$  versus 6-mo-old untreated mice, Tukey post-hoc test; •••,  $p < 0.001$  versus 6-mo-old untreated mice, Student's *t*-test.

DOI: 10.1371/journal.pmed.0020355.g005

transgenic and nontransgenic siblings using four-beam frames designed to monitor ambulation within an enclosed cage. As shown in Figure 7, the double transgenic mice were up to 10-fold more active during the dark phase of the day-night cycle than any of the control groups. Activity levels appeared to follow a relatively normal diurnal cycle, decreasing substantially during the daylight hours. However, even during the light phase, the tTA/APP mice remained many-fold more active than normal controls. This behavior was partially, but not consistently, reversed by 1 mo of transgene suppression beginning at 4–5 mo of age (data not shown). In contrast, hyperactivity was completely abolished by rearing tTA/APP mice on dox. Animals born and raised on dox showed activity levels similar to the untreated controls (Figure 7C). Intriguingly, all of the dox-reared animals, both transgenic and wild-type, showed altered circadian rhythms with far less distinction between their day- and nighttime activity levels.

## Discussion

We present a new mouse model for AD that was designed to test the consequences of inhibiting Aβ production after the onset of amyloid pathology. New lines of transgenic mice were developed for this study that express high levels of APP<sup>swE/ind</sup> under the control of a tetracycline-responsive promoter. We demonstrate that treatment with dox suppresses steady-state levels of both APP<sup>swE/ind</sup> and its C-terminal fragments, indicating that the mutant proteins have a relatively short half-life in vivo. Transgenic expression of APP<sup>swE/ind</sup> and consequent overproduction of Aβ42 cause early-onset amyloid deposition in untreated mice, in which deposits appear as early as 2 mo of age. Amyloid burden worsens significantly with age, and by 9 mo, the hippocampus and cortex of untreated mice are largely filled with aggregated peptide. We find that suppression of transgenic APP by more than 95% abruptly halts the progression of amyloid pathology. Importantly, this outcome occurs in animals already harboring considerable amyloid pathology, a situation similar to what might be expected in patients to be treated with secretase inhibitors. Somewhat unexpectedly, we observe no appreciable clearance of deposited amyloid even following periods of transgene suppression equal to the time taken for plaques to form. This latter finding indicates that compared to other disease-associated protein aggregates such as mutant huntingtin, which clear in less than 3 mo [32], the disaggregation of extracellular amyloid is relatively slow.

Notably, pharmaceutical γ-secretase inhibitors published to date show less strict regulation of Aβ production following chronic administration than we have attained here. Two independent compounds tested in Tg2576 [33] and TgCRND8



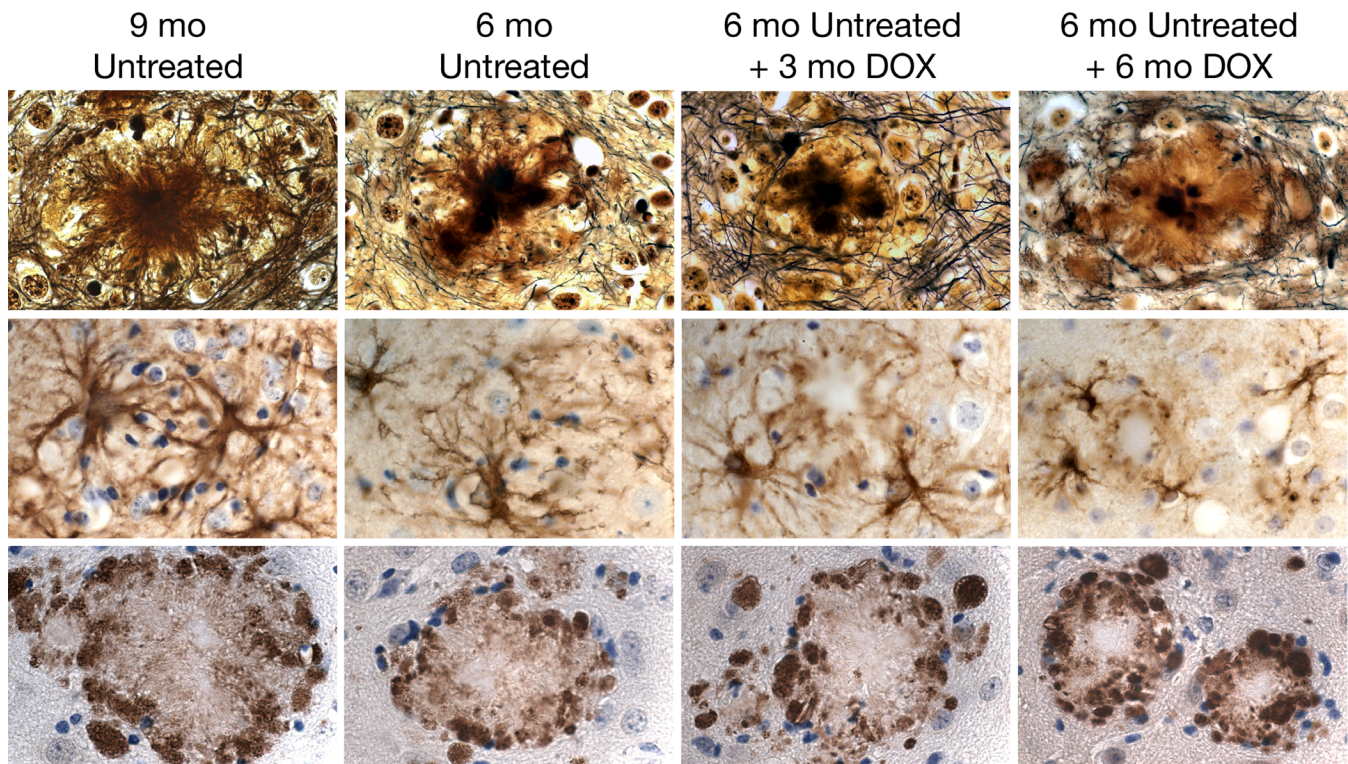


**Figure 6.** Neuritic and Glial Pathology Are Unchanged following Transgene Suppression

Dystrophic neurites and activated astrocytes surround most compact plaques in tet-off APP mice (line 107). Dark-stained, ubiquitin-filled neurites and reactive astrocytes form a halo around cored, fibrillar deposits by 6 mo of age that worsens with time in untreated mice. Both plaque-associated pathologies are arrested, although not reversed, by transgene suppression. Hirano silver stain (top row); GFAP immunohistochemistry (middle row); ubiquitin immunohistochemistry (bottom row).

DOI: 10.1371/journal.pmed.0020355.g006

[34] transgenic mice show no more than 85% suppression of A $\beta$ 40 levels, and where measured, even less suppression of A $\beta$ 42 (approximately 60%) [35,36]. Thus, even after accounting for the much higher APP expression levels in our mice than in the Tg2576 and TgCRND8 lines, we have achieved better absolute suppression of A $\beta$  production with the tet-off system than is currently possible with published  $\gamma$ -secretase inhibitors. Since even the most advanced future pharmaceutical agents are unlikely to attain more complete control of A $\beta$  production than achieved here, this system provides a salient test of therapeutic intervention with A $\beta$ -lowering compounds.

Although the progression of amyloid deposition was sharply arrested by this approach, we found that a substantial amyloid burden remained even after long periods of transgene suppression. We examined a small number of animals after 12 mo of dox treatment (beginning at 6 mo of age), and found that amyloid deposits were still relatively abundant. Longer-term treatments are now in progress. At the latest treatment interval analyzed by ELISA, animals administered dox for 6 mo showed elevated levels of PBS-soluble A $\beta$  (see Figure 5) that could be interpreted as an indication that the plaques are slowly releasing peptide (or oligomeric A $\beta$ ) into the soluble pool and might eventually dissolve. Whether inhibiting A $\beta$  production longer than 6 (or 12) mo may ultimately result in clearance of amyloid is under investigation; unfortunately, the life span of the model eventually limits this experiment. Therapeutics used in humans will have

considerably more time to act than is possible within the life span of rodent models. Long-term treatments would certainly be possible and could be a key to effective therapy. Overall, however, we interpret our findings as evidence that AD therapies that significantly lower the production of A $\beta$  (by either inhibiting secretase activity or inhibiting APP expression) may not quickly reverse preexisting pathology, but should effectively halt further deposition of amyloid.

In interpreting our study, it should be remembered that the earliest plaques to appear in these mice, like other APP transgenics harboring the Swedish mutation [27], are predominantly fibrillar deposits, which may be less tractable than the diffuse aggregates thought to come first in the course of the human disease. However, our data suggest that once diffuse deposits are formed in these mice, they are no more easily cleared in our system than cored plaques (see Figure S4). An additional consideration we recognize is that a small amount of transgene expression continues in the presence of dox and that endogenous mouse A $\beta$  continues to be produced. It is possible that the combined low levels of endogenous mouse A $\beta$  and nonsuppressed human peptide are sufficient to maintain existing deposits. However, these low levels of peptide are not sufficient to induce new amyloid formation, as CaMKII $\alpha$ -tTA  $\times$  tetAPP<sup>Swe/ind</sup> mice raised on dox for up to a year do not develop amyloid lesions (data not shown). It is also clear that in this genetic system, we have raised the production of A $\beta$  to levels not found in humans to accelerate pathology into an experimentally feasible time

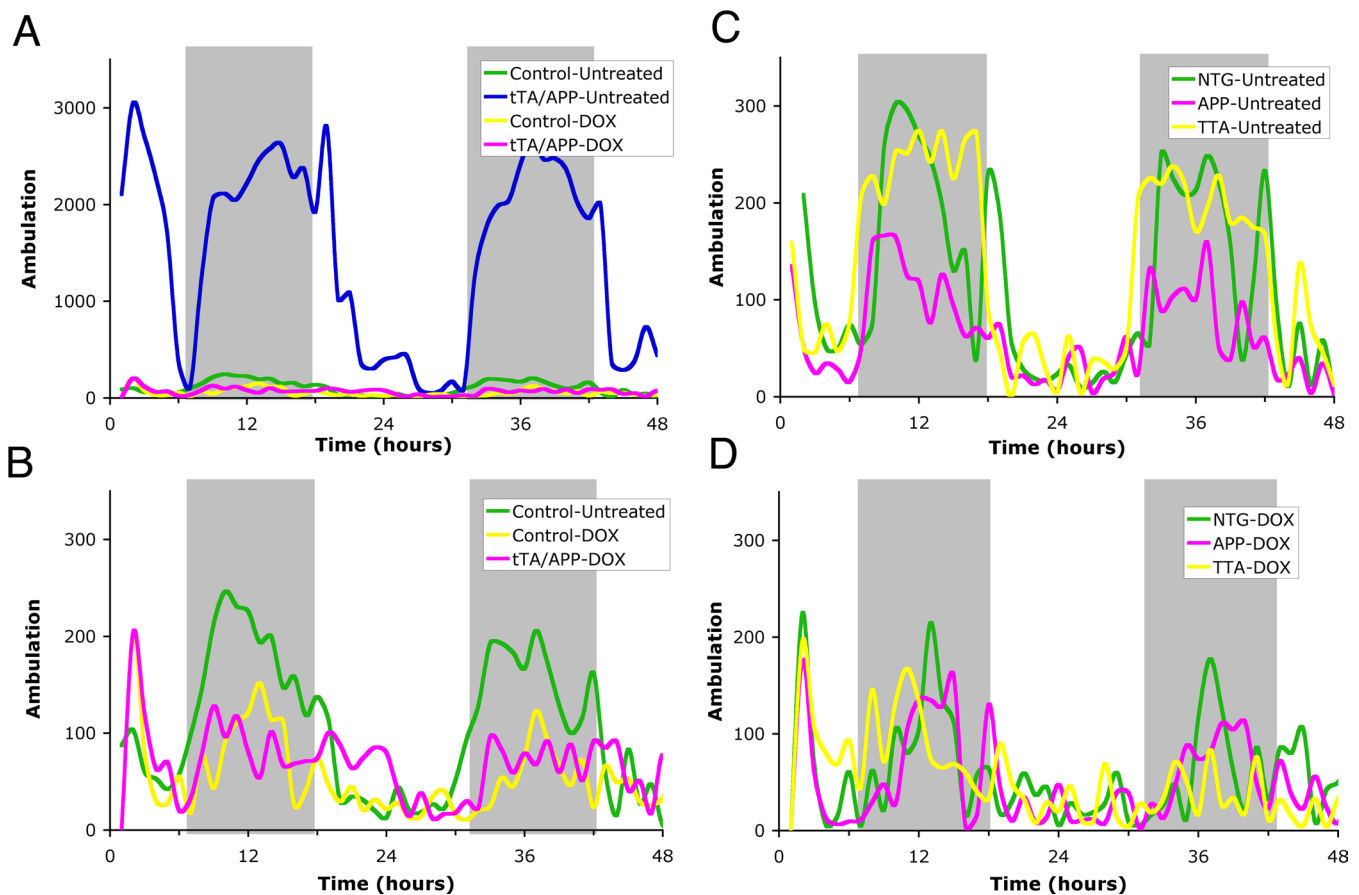


**Figure 7.** Transgene Suppression Attenuates Hyperactivity in tTA/APP Mice

(A) A 48-h measure of ambulation records extreme hyperactivity in untreated double transgenic mice compared to single transgenic and nontransgenic controls (line 107). This phenotype is completely eliminated by rearing the double transgenic mice on dox.

(B) The same data shown in (A) are replotted to magnify data from untreated control and dox-treated groups.

(C and D) Activity levels in the combined control groups of (A) and (B) are here separated by genotype. None of the single transgenic or nontransgenic control groups display the hyperactivity present in untreated tTA/APP animals. Again, note the y-axes have been enlarged for detail compared to (A). DOI: 10.1371/journal.pmed.0020355.g007

frame. This system allowed us to create an approximately 20-fold differential between APP/A $\beta$  synthetic rates before and after treatment, yet the *in vivo* equilibrium between aggregated and disaggregated states of A $\beta$  still favored the maintenance of amyloid deposits. In our opinion, it seems unlikely that amyloid deposits in human brain would be inherently any less stable than those formed in mouse brain. However, the human brain may harbor clearance mechanisms not shared by mice that would allow more efficient removal of preexisting amyloid.

One potential mechanism by which amyloid may be more efficiently removed in the human disease than in the mouse models is through microglial phagocytosis. Resident microglia in transgenic mouse models localize to tissue surrounding plaques but show little evidence of amyloid engulfment [37–40]. In contrast, microglia surrounding amyloid plaques in human brain show a much higher state of activation with greater expression of complement receptor [40]. Thus, the role of microglia in amyloid metabolism is minor in transgenic models compared to the human condition. Somewhat paradoxically, several studies further demonstrate that treatment with anti-inflammatory drugs to reduce microglial

activation actually lowers amyloid load in APP transgenic mice, suggesting a role for mouse microglia in the formation and maintenance of amyloid aggregates [41–43]. However, this outcome may be alternatively explained by direct effects of many anti-inflammatory drugs on  $\gamma$ -secretase cleavage [44–47]. Nonetheless, the role of microglia in both the human condition and the mouse models is poorly understood, and differences in microglial reactivity between the two could lead to significantly faster amyloid clearance in the brains of patients with AD than we observe in the tet-off APP mice.

Given the relatively minor role played by microglia in other mouse models of amyloidosis, we think it unlikely that these cells have influenced the rate of amyloid clearance in the tet-off APP mice. Even so, we considered the possibility that chronic dox treatment may have altered the activation state of microglia in our treated mice. Dox is structurally similar to minocycline, a reported anti-inflammatory drug and inhibitor of microglial activation [48]. However, if dox does have anti-inflammatory activity, then, based on previous studies with other anti-inflammatories, we would have expected to find less amyloid in the dox-treated animals. Clearly, that was not the case. While it is possible that dox acts in some other



way to slow amyloid clearance, data from multiple studies demonstrate that microglial responses are normally weak in the mouse AD models [37–40], and thus it is doubtful that dox-mediated microglial inhibition affected the outcome of our study.

The persistence and stability of amyloid deposits in our system is unexpected given the speed with which A $\beta$  aggregates are cleared in other mouse models of therapeutic intervention. Anti-A $\beta$  antibodies injected directly into the brain have been shown to eliminate amyloid deposits in as little as 1 wk after treatment [49–51]. Peripheral antibody injection decreases amyloid load more broadly, and although it does not appear to act as quickly as local injection, can significantly reduce amyloid load within 2 mo of initial treatment [52,53]. More recently, an alternative approach has shown that lentiviral transfer of neprilysin can also reduce the number of aggregates in the area of the injection site [54]. Careful study of the mechanism behind several of the antibody-mediated therapies has suggested that activated microglia play an important role in the removal of fibrillar plaques after immunization [50,52,55]. However, it has been noted that deletion of the Fc receptor (the primary receptor for microglial opsonization of antibody–antigen complexes) in APP transgenic mouse models has no impact on the effectiveness of antibody-mediated therapy [56,57]. It is, nevertheless, possible that lack of microglia activation is the major difference between the slow clearance described here, where no perturbation of the immune system is expected, and the rapid clearance described in studies involving antibody or viral injection. In isolation, mild activation of microglia by injection damage or opsonization may not be adequate to induce substantial phagocytosis, but when combined with an A $\beta$ -lowering agent, such as neprilysin or A $\beta$ -targeted antibodies, the two may work in concert to clear peptide deposits. Consistent with this hypothesis, strong activation of microglia through transgenic expression of TGF $\beta$  [58] or central injection of lipopolysaccharide [59,60] can by itself substantially reduce plaque burden in APP transgenic mice. But in the case of acute antibody- and/or injury-mediated activation, once the inflammation has passed, and the antibody and bound peptide have been cleared and degraded, the remaining A $\beta$  quickly reaggregates and amyloid pathology is reestablished [49]. This finding reinforces the notion that without continued stimulation, microglia in mouse models do not maintain the same level of sustained activation that may occur in humans.

SantaCruz et al. recently published a study of mice that express P301L human tau via a similar vector system [61]. As in our tet-off APP mice, SantaCruz et al. found that tau neurofibrillary tangles, like amyloid plaques, are not cleared efficiently following transgene suppression. The lack of clearance in both models of AD pathology comes as a stark contrast to the rapid removal of protein aggregates found in similar tet-off mouse models of Huntington [32] and prion disease [62]. In these cases, disrupting the input of new monomer to the system via dox-mediated transgene suppression led to relatively rapid clearance of protein aggregates. By contrast, our study and that of SantaCruz et al. suggest that protein aggregates in AD may be more tenacious than in other neurodegenerative disorders. Perhaps once aggregated, A $\beta$  and tau are either inherently more stable than other

protein aggregates or more resistant to intra- and extracellular clearance mechanisms.

One question we were not able to address in this study is whether abrogating synthesis of new A $\beta$  halts the progression of cognitive decline. Studies from the tet-off tau mice suggest that protein clearance may in fact not be required for cognitive improvement following transgene suppression [61]. At present, because of unexpected noncognitive behavioral abnormalities, it is not clear whether the tet-off APP mice can be used to address the same question in the context of amyloid pathology. Both lines of tTA/APP mice we studied here display extreme hyperactivity visible as cage circling and quantified by activity monitoring (see Figure 7). Many of the double transgenic mice showed similar circular patterns of swimming near the edge of the tank when tested in the Morris water maze. Expression of this phenotype makes standard tests of learning and memory uninterpretable. Hyperactivity nonspecifically inhibits choice-driven changes in movement, the key element behind all cognitive behavioral paradigms. We are currently working to determine whether hyperactivity correlates with expression of the APPsw/ind holoprotein or its proteolytic derivatives. Preliminary studies suggest that hyperactivity does not appear quickly when dox-reared mice are shifted to nonmedicated diets (J. L. J., unpublished data). These data may indicate that the neuroactive culprit is not immediately present after transgenic APP synthesis is initiated, but requires additional time to develop. Alternatively, hyperactivity may be caused by neuronal alterations due to transgene expression during early postnatal development. Further experiments are needed to distinguish between these possibilities.

In summary, we demonstrate that abrogating A $\beta$  production halts the progression of pathologic changes in a transgenic mouse model of Alzheimer-type amyloidosis. However, despite dramatic reductions in A $\beta$  synthesis, neuritic plaques are stable structures in vivo that do not quickly disaggregate. It is possible that a combination of therapies to limit A $\beta$  production, increase A $\beta$  degradation, and enhance phagocytosis of deposited amyloid may be required to reverse damage associated with AD. However, if started early enough in the course of disease, secretase inhibitors alone could provide substantial benefit in slowing pathogenic processes linked to amyloid deposition. Even at later stages in the disease, the presence of substantial microglial activation in human AD [40] suggests that simply slowing the formation of new amyloid deposits may allow ongoing phagocytosis to diminish preexisting lesions. However, the development of safe and effective secretase inhibitors will ultimately be required to determine whether the human brain has the capacity to repair amyloid-associated damage of AD once the progression of pathology is arrested.

## Supporting Information

**Figure S1.** Transgenic APP Expression and Suppression by Dox in the Four New Tet-Off APP Lines

Western blotting with human-specific antibody 6E10 reveals transgene-derived full-length APP in cortical homogenates from untreated animals (left lanes of each panel). The new lines produce exceptionally high levels of transgene expression; an equal amount of brain homogenate from a standard transgenic APP line is shown for comparison (extreme left lane, Standard Tg line C3–3; [15,63]). After

1 mo of dox treatment, transgenic protein in all four new tet-off APP lines is reduced to residual levels (+ dox; right lanes of each panel).

DOI: 10.1371/journal.pmed.0020355.sg001 (474 KB TIF).

#### Figure S2. Transgenic APP mRNA Is Brain-Specific

A slot blot of mRNA harvested from various tissues in three of the four new tet-off APP lines and a nontransgenic control was used to examine transgenic mRNA expression. Hybridization is seen only in the brain; no signal above background is seen in any other tissue.

DOI: 10.1371/journal.pmed.0020355.sg002 (781 KB PSD).

#### Figure S3. Amyloid Pathology in the Cortex Reiterates That in the Hippocampus

Amyloid histology was performed on sections from line 107 double transgenic mice by Hirano silver stain (top row), thioflavin-S (middle row), and A $\beta$  immunohistochemistry (bottom row) to examine the persistence of pathology following transgene suppression. As in the hippocampus (see Figure 4 and text), the progression of amyloid pathology in the cortex worsens substantially between 6 and 9 mo of age in untreated mice. This progression is completely prevented by suppression of the transgene with dox. For comparison, normal neurohistology is shown in an age-matched single transgenic (tTA only) animal. No amyloid pathology has been detected in either APP or tTA single transgenic animals up to 15 mo of age.

DOI: 10.1371/journal.pmed.0020355.sg003 (4.8 MB PSD).

#### Figure S4. Diffuse Deposits Do Not Disperse During A $\beta$ Suppression

Campbell-Switzer silver stain was used to differentiate cored (brown) from diffuse (black) deposits in line 107 tTA/APP mice. This stain demonstrates that both types of deposit persist throughout long periods of transgene suppression. The lower panels, showing low-power images (10 $\times$ ) of frontal cortex from each condition, reveal little change in the extent of diffuse amyloid following up to 6 mo of A $\beta$  suppression. High-power images (40 $\times$ ) in the upper panels show that the diffuse halo surrounding individual cored deposits remains relatively unchanged in treated mice. Untreated tTA single transgenic animals are shown as a negative control. Protocol for the Campbell-Switzer Alzheimer's Method was kindly shared by Robert Switzer, III (NeuroScience Associates, Knoxville, Tennessee, United States), and can be downloaded at [http://www.nsalabs.com/Documents/publications/campbell-switzer\\_protocol.htm](http://www.nsalabs.com/Documents/publications/campbell-switzer_protocol.htm) [64,65].

DOI: 10.1371/journal.pmed.0020355.sg004 (923 KB JPG).

#### Figure S5. Chronic Transgene Suppression and Arrest of A $\beta$ Aggregate Formation in an Independent Line of Tet-Off APP Mice (CaMKII $\alpha$ -tTA $\times$ tet-APP<sup>swe/ind</sup> Line 18)

(A) The experiment presented in the text for line 107 tet-off APP was repeated with a second tet-off APP line (line 18) to control for integration site artifacts. Cortical homogenates from untreated control and dox-treated double transgenic mice were immunoblotted for full-length APP with the human-specific antibody 6E10 to confirm transgene suppression at the time of harvest. Immunostaining for endogenous superoxide dismutase (SOD1) was included as a loading control.

(B) Quantitation of signal intensity from the Western blot in (A) shows transgenic APP levels in line 18 are suppressed by more than 98% following 3 mo of dox treatment (significant effect of group ANOVA  $F_{2,8} = 1559.7$ ,  $p < 0.001$ ). This level of suppression was equal to or better than that attained in line 107 (see Figure 3B).

(C) Serial dilution filter trap assay was used to quantify aggregated A $\beta$  in cortical homogenates.

(D) Quantitation of signal intensity in the linear range of the dilution series shown in (C). Consistent with the amyloid histology shown in Figure S5, aggregate formation was significantly increased between 6 and 9 mo of age in untreated mice (significant effect of group ANOVA  $F_{2,18} = 12.14$ ,  $p < 0.001$ ). Aggregate formation was completely arrested by transgene suppression, and is identical in 9-mo-old mice treated with dox for 3 mo as in untreated animals harvested when treatment began ( $p > 0.5$ , Tukey post-hoc test). \*,  $p < 0.05$ ; \*\*,  $p < 0.005$ ; \*\*\*,  $p < 0.001$  versus 9-mo-old untreated mice, Tukey post-hoc test.

DOI: 10.1371/journal.pmed.0020355.sg005 (962 KB TIF).

#### Figure S6. Arrest of Amyloid Progression by Chronic Transgene Suppression in Line 18 Tet-Off APP Mice

Amyloid histology in cortical (first and third rows) and hippocampal (second and fourth rows) sections from untreated tTA/APP mice shows a dramatic progression of pathology between 6 and 9 mo of age. Suppression of transgenic APP expression arrests this progres-

sion, although without any sign of plaque clearance (6 mo + 3 mo dox). Hirano silver stain (top panels); thioflavin-S (bottom panels).

DOI: 10.1371/journal.pmed.0020355.sg006 (5.8 MB PSD).

## Acknowledgments

We thank Patrick Tremblay for helpful advice on the tet system at a critical time in the project, and Mark Mayford for sharing the CaMKII $\alpha$ -tTA mice through Jackson Laboratory. We also thank Fraser Moss for saving several immunoblots with last-minute shipments, Andy Groves for many thoughtful discussions, Neil Segil for generously sharing his laboratory and equipment, Beth Olson, Natasha Bouey, and Yolanda Jackson for outstanding animal care, Debbie Swing for expert microinjection, and Dave Fromholt for genotyping and dissection. We gratefully acknowledge Takeda Chemical Industries for providing antibodies BAN50, BA27, and BC05, Konrad Beyreuther and Andreas Weidemann for providing 22C11 antibody, and Ed Koo for sharing CT15 antibody. This work was supported by grants from the Johns Hopkins Alzheimer's Disease Research Center (JLJ), the National Alliance for Research on Schizophrenia and Depression (Young Investigator Award [JLJ]), the Rose Hills Foundation (JLJ), the Alzheimer's Association (Zenith Award [DRB]), the National Institute of Aging (K01 AG26144-01 [JLJ], P50 AG05146-20 [DRB], R01 AG006656-16 [SGY], and P01 AG015453 [SGY]), the National Institute of Neurologic Disease and Stoke (R01 NS 047225 [DRB]), and the National Cancer Institute (NAJ and NGC). The funding agencies generously provided for research supplies, animal care, and salary support; the funders of this work had no role in study design, data collection and analysis, decision to publish, or preparation of the manuscript.

## References

- Hardy JA, Higgins GA (1992) Alzheimer's disease: The amyloid cascade hypothesis. *Science* 256: 184–185.
- Selkoe DJ, Podlisny MB (2002) Deciphering the genetic basis of Alzheimer's disease. *Annu Rev Genomics Hum Genet* 3: 67–99.
- Rademakers R, Cruts M, Van Broeckhoven C (2003) Genetics of early-onset Alzheimer dementia. *ScientificWorldJournal* 3: 497–519.
- Orgogozo JM, Gilman S, Dartigues JF, Laurent B, Puel M, et al. (2003) Subacute meningoencephalitis in a subset of patients with AD after A $\beta$ 42 immunization. *Neurology* 61: 46–54.
- Check E (2002) Nerve inflammation halts trial for Alzheimer's drug. *Nature* 415: 462.
- Hock C, Konietzko U, Streffer JR, Tracy J, Signorell A, et al. (2003) Antibodies against  $\beta$ -amyloid slow cognitive decline in Alzheimer's disease. *Neuron* 38: 547–554.
- Nicoll JA, Wilkinson D, Holmes C, Steart P, Markham H, et al. (2003) Neuropathology of human Alzheimer disease after immunization with amyloid- $\beta$  peptide: A case report. *Nat Med* 9: 448–452.
- Tsai JY, Wolfe MS, Xia W (2002) The search for  $\gamma$ -secretase and development of inhibitors. *Curr Med Chem* 9: 1087–1106.
- Wolfe MS (2002) Therapeutic strategies for Alzheimer's disease. *Nat Rev Drug Discov* 1: 859–866.
- Cumming JN, Iserloh U, Kennedy ME (2004) Design and development of BACE-1 inhibitors. *Curr Opin Drug Discov Devel* 7: 536–556.
- Citron M (2004)  $\beta$ -secretase inhibition for the treatment of Alzheimer's disease—Promise and challenge. *Trends Pharmacol Sci* 25: 92–97.
- Gossen M, Bujard H (1992) Tight control of gene expression in mammalian cells by tetracycline-responsive promoters. *Proc Natl Acad Sci U S A* 89: 5547–5551.
- Furth PA, St Onge L, Boger H, Gruss P, Gossen M, et al. (1994) Temporal control of gene expression in transgenic mice by a tetracycline-responsive promoter. *Proc Natl Acad Sci U S A* 91: 9302–9306.
- Kistner A, Gossen M, Zimmermann F, Jerecic J, Ullmer C, et al. (1996) Doxycycline-mediated quantitative and tissue-specific control of gene expression in transgenic mice. *Proc Natl Acad Sci U S A* 93: 10933–10938.
- Borchelt DR, Davis J, Fischer M, Lee MK, Slunt HH, et al. (1996) A vector for expressing foreign genes in the brains and hearts of transgenic mice. *Genet Anal* 13: 159–163.
- Mayford M, Bach ME, Huang YY, Wang L, Hawkins RD, et al. (1996) Control of memory formation through regulated expression of a CaMKII transgene. *Science* 274: 1678–1683.
- Weidemann A, König G, Bunke D, Fischer P, Salbaum JM, et al. (1989) Identification, biogenesis, and localization of precursors of Alzheimer's disease A4 amyloid protein. *Cell* 57: 115–126.
- Borchelt DR, Lee MK, Slunt HS, Guarnieri M, Xu ZS, et al. (1994) Superoxide dismutase 1 with mutations linked to familial amyotrophic lateral sclerosis possesses significant activity. *Proc Natl Acad Sci U S A* 91: 8292–8296.
- Sisodia SS, Koo EH, Hoffman PN, Perry G, Price DL (1993) Identification and transport of full-length amyloid precursor proteins in rat peripheral nervous system. *J Neurosci* 13: 3136–3142.

20. Church GM, Gilbert W (1984) Genomic sequencing. *Proc Natl Acad Sci U S A* 81: 1991–1995.
21. Yamamoto T, Hirano A (1986) A comparative study of modified Bielschowsky, Bodian and thioflavin S stains on Alzheimer's neurofibrillary tangles. *Neuropathol Appl Neurobiol* 12: 3–9.
22. Xu G, Gonzales V, Borchelt DR (2002) Rapid detection of protein aggregates in the brains of Alzheimer patients and transgenic mouse models of amyloidosis. *Alzheimer Dis Assoc Disord* 16: 191–195.
23. Kawarabayashi T, Younkin LH, Saido TC, Shoji M, Ashe KH, et al. (2001) Age-dependent changes in brain, CSF, and plasma amyloid  $\beta$  protein in the Tg2576 transgenic mouse model of Alzheimer's disease. *J Neurosci* 21: 372–381.
24. Suzuki N, Cheung TT, Cai XD, Odaka A, Otvos L Jr, et al. (1994) An increased percentage of long amyloid  $\beta$  protein secreted by familial amyloid  $\beta$  protein precursor (BAPP717) mutants. *Science* 264: 1336–1340.
25. Gravina SA, Ho L, Eckman CB, Long KE, Otvos L Jr, et al. (1995) Amyloid  $\beta$  protein ( $A\beta$ ) in Alzheimer's disease brain. Biochemical and immunocytochemical analysis with antibodies specific for forms ending at A $\beta$ 40 or A $\beta$ 42(43). *J Biol Chem* 270: 7013–7016.
26. Jankowsky JL, Fadale DJ, Anderson J, Xu GM, Gonzales V, et al. (2004) Mutant presenilins specifically elevate the levels of the 42 residue  $\beta$ -amyloid peptide in vivo: Evidence for augmentation of a 42-specific  $\gamma$ -secretase. *Hum Mol Genet* 13: 159–170.
27. Borchelt DR, Ratovitski T, van Lare J, Lee MK, Gonzales V, et al. (1997) Accelerated amyloid deposition in the brains of transgenic mice coexpressing mutant presenilin 1 and amyloid precursor proteins. *Neuron* 19: 939–945.
28. Herms J, Zurmohle U, Brysch W, Schlingensiepen KH (1993) Ca<sup>2+</sup>/calmodulin protein kinase and protein kinase C expression during development of rat hippocampus. *Dev Neurosci* 15: 410–416.
29. Phinney AL, Deller T, Stalder M, Calhoun ME, Frotscher M, et al. (1999) Cerebral amyloid induces aberrant axonal sprouting and ectopic terminal formation in amyloid precursor protein transgenic mice. *J Neurosci* 19: 8552–8559.
30. Kotilinek LA, Bacskai B, Westerman M, Kawarabayashi T, Younkin L, et al. (2002) Reversible memory loss in a mouse transgenic model of Alzheimer's disease. *J Neurosci* 22: 6331–6335.
31. Savonenko A, Xu GM, Melnikova T, Morton JL, Gonzales V, et al. (2005) Episodic-like memory deficits in the APPsw/PS1dE9 mouse model of Alzheimer's disease: Relationships to  $\beta$ -amyloid deposition and neurotransmitter abnormalities. *Neurobiol Dis* 18: 602–617.
32. Yamamoto A, Lucas JJ, Hen R (2000) Reversal of neuropathology and motor dysfunction in a conditional model of Huntington's disease. *Cell* 101: 57–66.
33. Hsiao K, Chapman P, Nilsen S, Eckman C, Harigaya Y, et al. (1996) Correlative memory deficits,  $A\beta$  elevation, and amyloid plaques in transgenic mice. *Science* 274: 99–102.
34. Chishti MA, Yang DS, Janus C, Phinney AL, Horne P, et al. (2001) Early-onset amyloid deposition and cognitive deficits in transgenic mice expressing a double mutant form of amyloid precursor protein 695. *J Biol Chem* 276: 21562–21570.
35. Wong GT, Manfra D, Poulet FM, Zhang Q, Josien H, et al. (2004) Chronic treatment with the gamma-secretase inhibitor LY-411,575 inhibits  $\beta$ -amyloid peptide production and alters lymphopoiesis and intestinal cell differentiation. *J Biol Chem* 279: 12876–12882.
36. Barten DM, Guss VL, Corsa JA, Loo A, Hansel SB, et al. (2005) Dynamics of  $\beta$ -amyloid reductions in brain, cerebrospinal fluid, and plasma of  $\beta$ -amyloid precursor protein transgenic mice treated with a  $\gamma$ -secretase inhibitor. *J Pharmacol Exp Ther* 312: 635–643.
37. Sasaki A, Shoji M, Harigaya Y, Kawarabayashi T, Ikeda M, et al. (2002) Amyloid cored plaques in Tg2576 transgenic mice are characterized by giant plaques, slightly activated microglia, and the lack of paired helical filament-typed, dystrophic neurites. *Virchows Arch* 441: 358–367.
38. Wegiel J, Imaki H, Wang KC, Wegiel J, Rubenstein R (2004) Cells of monocyte/microglial lineage are involved in both microvessel amyloidosis and fibrillar plaque formation in APPsw tg mice. *Brain Res* 1022: 19–29.
39. Wegiel J, Wang KC, Imaki H, Rubenstein R, Wronska A, et al. (2001) The role of microglial cells and astrocytes in fibrillar plaque evolution in transgenic APPsw mice. *Neurobiol Aging* 22: 49–61.
40. Schwab C, Hosokawa M, McGeer PL (2004) Transgenic mice overexpressing amyloid  $\beta$  protein are an incomplete model of Alzheimer disease. *Exp Neurol* 188: 52–64.
41. Jantzen PT, Connor KE, DiCarlo G, Wenk GL, Wallace JL, et al. (2002) Microglial activation and  $\beta$ -amyloid deposit reduction caused by a nitric oxide-releasing nonsteroidal anti-inflammatory drug in amyloid precursor protein plus presenilin-1 transgenic mice. *J Neurosci* 22: 2246–2254.
42. Lim GP, Yang F, Chu T, Chen P, Beech W, et al. (2000) Ibuprofen suppresses plaque pathology and inflammation in a mouse model for Alzheimer's disease. *J Neurosci* 20: 5709–5714.
43. Yan Q, Zhang J, Liu H, Babu-Khan S, Vassar R, et al. (2003) Anti-inflammatory drug therapy alters  $\beta$ -amyloid processing and deposition in an animal model of Alzheimer's disease. *J Neurosci* 23: 7504–7509.
44. Eriksen JL, Sagi SA, Smith TE, Weggen S, Das P, et al. (2003) NSAIDs and enantiomers of flurbiprofen target gamma-secretase and lower A $\beta$ 42 in vivo. *J Clin Invest* 112: 440–449.
45. Weggen S, Eriksen JL, Das P, Sagi SA, Wang R, et al. (2001) A subset of NSAIDs lower amyloidogenic A $\beta$ 42 independently of cyclooxygenase activity. *Nature* 414: 212–216.
46. Weggen S, Eriksen JL, Sagi SA, Pietrzik CU, Ozols V, et al. (2003) Evidence that nonsteroidal anti-inflammatory drugs decrease amyloid  $\beta$  42 production by direct modulation of  $\gamma$ -secretase activity. *J Biol Chem* 278: 31831–31837.
47. Lleo A, Bereznovska O, Herl L, Raju S, Deng A, et al. (2004) Nonsteroidal anti-inflammatory drugs lower A $\beta$ 42 and change presenilin 1 conformation. *Nat Med* 10: 1065–1066.
48. Yrjanheikki J, Keinänen R, Pellikka M, Hokfelt T, Koistinaho J (1998) Tetracyclines inhibit microglial activation and are neuroprotective in global brain ischemia. *Proc Natl Acad Sci U S A* 95: 15769–15774.
49. Oddo S, Billings L, Kesslak JP, Cribbs DH, LaFerla FM (2004) A $\beta$  immunotherapy leads to clearance of early, but not late, hyperphosphorylated tau aggregates via the proteasome. *Neuron* 43: 321–332.
50. Wilcock DM, DiCarlo G, Henderson D, Jackson J, Clarke K, et al. (2003) Intracranially administered anti-A $\beta$  antibodies reduce beta-amyloid deposition by mechanisms both independent of and associated with microglial activation. *J Neurosci* 23: 3745–3751.
51. Bacskai BJ, Kajdasz ST, Christie RH, Carter C, Games D, et al. (2001) Imaging of amyloid- $\beta$  deposits in brains of living mice permits direct observation of clearance of plaques with immunotherapy. *Nat Med* 7: 369–372.
52. Bard F, Cannon C, Barbour R, Burke RL, Games D, et al. (2000) Peripherally administered antibodies against amyloid  $\beta$ -peptide enter the central nervous system and reduce pathology in a mouse model of Alzheimer disease. *Nat Med* 6: 916–919.
53. Wilcock DM, Rojiani A, Rosenthal A, Levkowitz G, Subbarao S, et al. (2004) Passive amyloid immunotherapy clears amyloid and transiently activates microglia in a transgenic mouse model of amyloid deposition. *J Neurosci* 24: 6144–6151.
54. Marr RA, Rockenstein E, Mukherjee A, Kindy MS, Hersh LB, et al. (2003) Neprilysin gene transfer reduces human amyloid pathology in transgenic mice. *J Neurosci* 23: 1992–1996.
55. Wilcock DM, Munireddy SK, Rosenthal A, Ugen KE, Gordon MN, et al. (2004) Microglial activation facilitates A $\beta$  plaque removal following intracranial anti-A $\beta$  antibody administration. *Neurobiol Dis* 15: 11–20.
56. Das P, Howard V, Loosbrock N, Dickson D, Murphy MP, et al. (2003) Amyloid- $\beta$  immunization effectively reduces amyloid deposition in FcR $\gamma$ -knock-out mice. *J Neurosci* 23: 8532–8538.
57. Bacskai BJ, Kajdasz ST, McLellan ME, Games D, Seubert P, et al. (2002) Non-Fc-mediated mechanisms are involved in clearance of amyloid- $\beta$  in vivo by immunotherapy. *J Neurosci* 22: 7873–7878.
58. Wyss-Coray T, Lin C, Yan F, Yu GQ, Rohde M, et al. (2001) TGF $\beta$ 1 promotes microglial amyloid- $\beta$  clearance and reduces plaque burden in transgenic mice. *Nat Med* 7: 612–618.
59. DiCarlo G, Wilcock D, Henderson D, Gordon M, Morgan D (2001) Intrahippocampal LPS injections reduce A $\beta$  load in APP+PS1 transgenic mice. *Neurobiol Aging* 22: 1007–1012.
60. Herber DL, Roth LM, Wilson D, Wilson N, Mason JE, et al. (2004) Time-dependent reduction in A $\beta$  levels after intracranial LPS administration in APP transgenic mice. *Exp Neurol* 190: 245–253.
61. SantaCruz K, Lewis J, Spire T, Paulson J, Kotilinek L, et al. (2005) Tau suppression in a neurodegenerative mouse model improves memory function. *Science* 309: 476–481.
62. Safar JG, DeArmond SJ, Kociuba K, Deering C, Didorenko S, et al. (2005) Prion clearance in bigenic mice. *J Gen Virol*. In press.
63. Borchelt DR, Thinakaran G, Eckman CB, Lee MK, Davenport F, et al. (1996) Familial Alzheimer's disease-linked presenilin 1 variants elevate A $\beta$ 1–42/1–40 ratio in vitro and in vivo. *Neuron* 17: 1005–1013.
64. Campbell SK, Switzer RC, Martin TL (1987) Alzheimer's plaques and tangles: A controlled and enhanced silver staining method. *Soc Neurosci Abstr* 13: 189.9.
65. Switzer RC, Campbell SK, Murdock TM, inventors (1993 March 9) A histologic method for staining Alzheimer pathology. United States patent 5,192,688.

## Patient Summary

**Background** Patients with Alzheimer disease (AD) have elevated levels of a small protein called amyloid- $\beta$  peptide that sticks together to form what are known as amyloid plaques in their brains. This peptide is normally made at low levels in healthy individuals, and is made when a larger protein called amyloid precursor protein (APP) is cut down in size. New treatments are now being developed that will decrease the amount of A $\beta$  produced from APP. However, it is not clear whether lowering the production of A $\beta$  will allow the brain to heal itself by clearing the amyloid plaques. The answer to this question may be important for deciding when A $\beta$ -lowering drugs should be started, and may also determine how effective they are in reversing the mental symptoms of AD.

**What Did the Researchers Do and Find?** Because new drugs designed to lower A $\beta$  levels are still in development, they are not available for testing in animal models of the disease. Instead, basic questions about the effectiveness of this type of treatment must be answered using systems that mimic how the drugs work. To do this, the authors created mice that produce too much APP and that develop the same amyloid lesions as do human patients with AD. Unlike normal mice, these mice also carried a “switch” gene that allowed the researchers to turn off APP by feeding the mice special food. Turning off APP in these mice had the same effect as treating them with A $\beta$ -lowering drugs, and so the researchers were able to ask what happened to the amyloid plaques after A $\beta$  production was shut down. They showed that lowering A $\beta$  production prevents the amyloid lesions from getting worse as the disease progresses. This means that treatment with A $\beta$ -lowering drugs may be able to stop the disease from filling the brain with plaques. However, the researchers also found that the amyloid lesions that had formed before treatment was started remained intact throughout the experiment.

**What Do These Findings Mean?** These results indicate that treatments designed to lower the production of A $\beta$  may be an important part of future AD treatment, as this approach seems to prevent additional amyloid plaques from forming in the mouse brain. However, by itself, this strategy may not be able to rid the brain of plaques that have already formed in the brain before treatment is started. The findings suggest that early treatment may be important for this approach to succeed.

**Where Can I Get More Information Online?** MedlinePlus has several Web pages of information on Alzheimer disease:  
<http://www.nlm.nih.gov/medlineplus/alzheimersdisease.html>  
 The ADEAR Center of the US Government's National Institute on Aging also has information on Alzheimer disease:  
<http://www.alzheimers.org/>  
 The Alzheimer's Association Web site contains information on both caregiving and research:  
<http://www.alz.org>